Journal of Medicinal Chemistry

ARTICLE

pubs.acs.org/jmc

Highly Potent 5-Aminotetrahydropyrazolopyridines: Enantioselective Dopamine D_3 Receptor Binding, Functional Selectivity, and Analysis of Receptor−Ligand Interactions

Nuska Tschammer,[†] Jan Elsner,[†] Angela Goetz,[†] Katharina Ehrlich,[†] Stefan Schuster,[†] Miriam Ruberg,[†] Julia Kühhorn,[†] Dawn Thompson,[‡] Jennifer Whistler,[‡] Harald Hübner,[†] and Peter Gmeiner*[,†]

[†]Department of Chemistry and Pharmacy, Emil Fischer Center, Friedrich Alexander University, Schuhstrasse 19, D-91052 Erlangen, Germany

[‡]Ernest Gallo Clinic and Research Center and Department of Neurology, University of California—San Francisco, Emeryville, California 94608, United States

Supporting Information

ABSTRACT: Heterocyclic dopamine surrogates of types **5** and **7** were synthesized and investigated for their dopaminergic properties. The enantiomerically pure biphenylcarboxamide (*S*)-**5a** displayed an outstanding K_i of 27 pM at the agonist-labeled D_3 receptor and significant selectivity over the D_2 subtype. Measurement of [^{35}S]GTPγS incorporation in the presence of a coexpressed PTX-insensitive $G_{\alpha o-1}$ subunit indicated highly efficient G-protein coupling. Comparison of ligand efficacy data from cAMP accumulation and [^{3}H]thymidine incorporation experiments revealed that ligand biased signaling is exerted by the test compound (*S*)-**5a**. Starting from the D_3 crystal structure, a combination of homology modeling and site directed mutagenesis gave valuable insights into the binding mode and the intermolecular origins of stereospecific receptor recognition. According to these data, the superior affinity of the eutomer **5a** is caused by the favorable binding energy that results from interaction between the ligand's central ammonium unit and the aspartate residue in position 3.32 of the receptor.

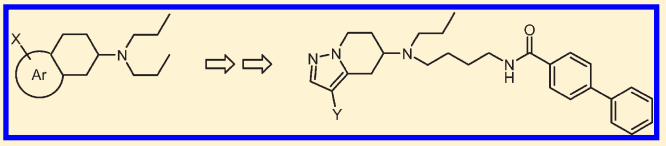

INTRODUCTION

Dopamine receptors are phylogenetically classified into D_1 and D_5 as well as D_2, D_3, and D_4 subtypes coupling to the G proteins G_s and $G_{i/o}$, respectively.[1] Substantial attenuation of dopaminergic neurotransmission caused by gradual loss of dopaminergic neurons in the pars compacta of the substantia nigra leads to chronic progressive Parkinson's disease.[2] A common pharmacotherapy used for the treatment of Parkinson's disease is the dopamine precursor levodopa (L-dopa).[2,3] Long-term use of L-dopa often results in a reduced treatment efficacy, motor fluctuations with dyskinesia, and psychological disturbances including hallucinations.[4] Dopamine receptor agonists that target D_2 and D_3 dopamine receptors have been successfully used to replace dopamine. Some neuroprotective effects have been reported for D_3-preferring agonists during the early stages of Parkinson's disease.[5−7] Because of the lack of highly selective D_2 and D_3 receptor agonists, it is not clear if subtype specific stimulation may be advantageous over simultaneous D_2/D_3 receptor activation. The question, which pattern of intrinsic activities may be the most beneficial for the treatment of Parkinson's disease, remains.

Complementing the classical D_2/D_3 agonists of type **1** representing conformationally restricted dopamine analogues and heterocyclic bioisosteres thereof,[8−11] *N*-butyl-4-biphenylcarboxamido substituted phenylpiperazines including the derivative **2** were reported as selective D_3 partial agonists (Chart 1).[12−14] We have shown that ferrocene analogues of **2** behave as neutral antagonists at the dopamine receptors D_3 and D_4 and as partial agonists at the D_2 subtype (intrinsic activity of 57%, EC_{50} = 2.5 nM).[15] Incorporating enyne-derived headgroups as nonaromatic catechol bioisosteres, we could furthermore demonstrate that *N*-butyl-4-biphenylcarboxamides exhibit ligand biased signaling (functional selectivity) when compared to their dipropylamine substituted congeners.[16] The long-chain analogues have been more efficacious in the D_3 receptor mediated [^{3}H]thymidine incorporation (mitogenesis) compared to a substantially lower efficacy in the inhibition of cAMP accumulation.[16]

As an extension of recent investigations,[11,17,18] we have studied a formal structural hybridization of dopaminergic dipropylamines of type **1** with partial agonists of type **2** leading to molecular probes of type **3**. To design novel dopaminergic chemotypes displaying potentially higher binding affinity, we envisaged a start from our previously described 5-aminotetrahydropyrazolopyridines **4**[19] and the tricyclic ergoline analogues **6** as lead structures and transformed them into the novel target compounds of types **5** and **7**, respectively. Herein, we describe

Received: December 23, 2010
Published: March 09, 2011

Chart 1. Structural Hybridization of Dopaminergic Dipropylamines and Arenecarboxamides

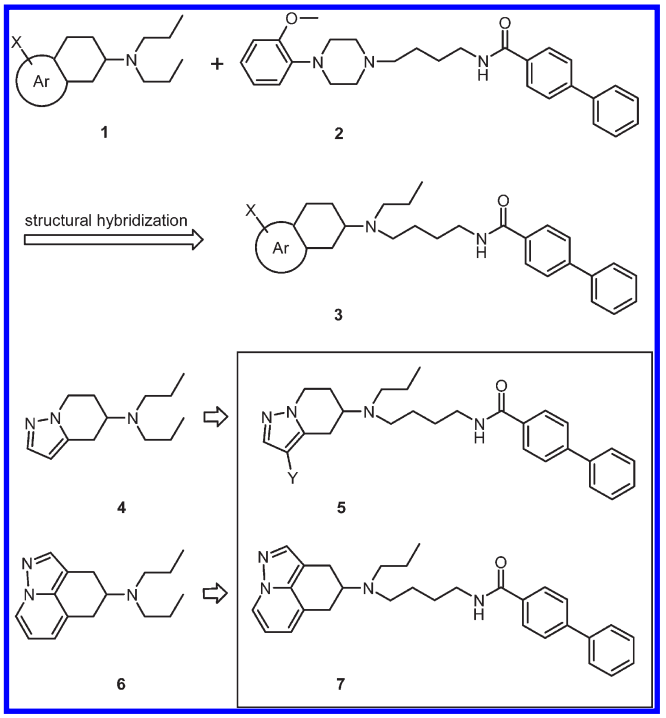

Scheme 1[a]

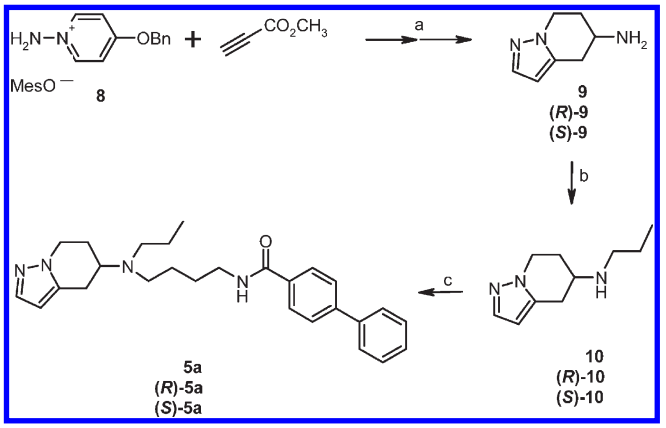

[a] Reagents and conditions: (a) ref 19; (b) propionaldehyde, $NaBH_3CN$, MeOH, 0 °C, 45 min (68%); (c) 4-(4-phenylbenzoylamino)butyraldehyde, $NaBH(OAc)_3$, 1,2-dichloroethane, room temp, 18 h (87%).

the chemical synthesis of these "long chain analogues", receptor binding studies, and functional activity profiles in assays measuring the D_{2long} and D_3 receptor mediated incorporation of [^{35}S]GTPγS, inhibition of cAMP accumulation, and stimulation of [^{3}H]thymidine incorporation (mitogenesis). Additionally, we investigated the ability of novel compounds to induce the D_{2long} receptor internalization. The phenylpiperazine **2** and the pure enantiomers of the dipropylamine substituted heterocycle **4** served as reference agents. To better understand the binding mode of our test compounds, mutagenesis experiments and docking studies based on the recent crystal structure of D_3[20] were performed.

Scheme 2[a]

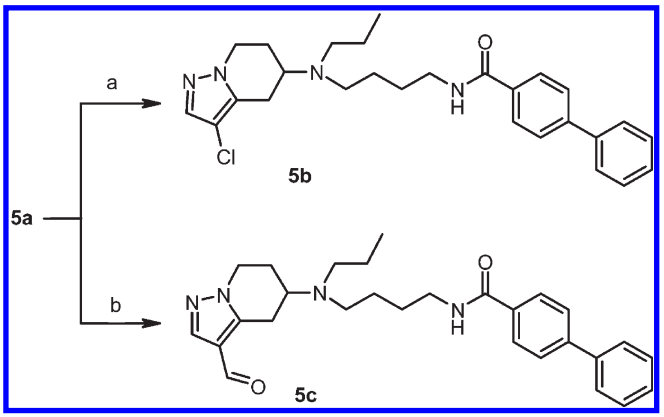

[a] Reagents and conditions: (a) NCS, $CHCl_3$, reflux, 16 h (69%); (b) $POCl_3$, DMF, 90 °C, 2 h (65%).

Scheme 3[a]

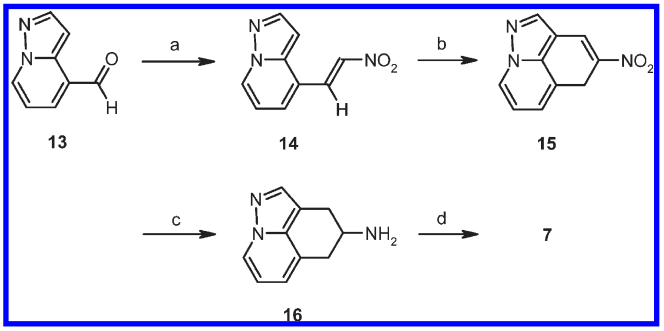

[a] Reagents and conditions: (a) CH_3NO_2, $CH_3NH_2 \cdot HCl$, CH_3COOK, MeOH, room temp, 3 days (80%); (b) (1) $NaBH_3(CN)$, MeOH, 0 °C, 40 min (82%); (2) $POCl_3$, DMF, 0 °C, 15 min, room temp, 15 min, H_2O/DMF, 0 °C, 15 min, Et_3N, MeOH, room temp, 15 min (51%); (c) (1) $NaBH_4$, MeOH, room temp, 40 min (81%); (2) tin powder, acetic acid, EtOH, room temp, 3 days (65%); (d) (1) propionaldehyde, $NaCNBH_3$, MeOH, 0 °C, 45 min, (53%); (2) 4-(4-phenylbenzoylamino)butyraldehyde, $NaBH(OAc)_3$, 1,2-dichloroethane, room temp, 18 h (87%).

RESULTS AND DISCUSSION

Synthesis. Fused pyrazole derivatives have been described as excellent molecular scaffolds in dopaminergic bi- and tricyclic ergoline analogues.[18,19,21,22] Efficient synthetic pathways to the fused pyrazole derivatives of types **5** and **7** were elaborated. Starting from *N*-amino-4-benzyloxypyridinium mesitylene sulfonate **8**, we followed our previously described protocol involving 1,3-dipolar cycloaddition with methyl propiolate under oxidative conditions, simultaneous cleavage of the benzyl ether function, removal of the carboxylic ester group, catalytic hydrogenation, activation of the secondary alcohol, nucleophilic displacement with sodium azide, and subsequent reduction to afford the primary amine **9** in racemic form (Scheme 1). To prepare the pure enantiomers (*R*)-**9** and (*S*)-**9**, the primary amino group of **9** was reacted with (−)-menthyl chloroformate, resulting in a mixture of the diastereomeric carbamates that were chromatographically separated and cleaved under hydrolytic conditions. N-Monopropylation of **9** was accomplished upon reaction of **9**, (*R*)-**9** and (*S*)-**9**, with propionaldehyde and $NaBH_3CN$ at 0 °C

dx.doi.org/10.1021/jm101639t |*J. Med. Chem.* 2011, 54, 2477–2491

when a reaction time of 45 min was crucial to success. The thus formed secondary amines **10**, (*S*)-**10** and (*R*)-**10**, were reductively alkylated with 4-(4-phenylbenzoylamino)butyraldehyde[23] in the presence of $NaBH(OAc)_3$ to give rise to the test compounds **5a**, (*R*)-**5a** and (*S*)-**5a**, respectively. Preparative HPLC employing a chiral column gave an alternative access to (*R*)-**5a** and (*S*)-**5a** via separation of racemic material. To investigate if the biphenylcarboxamides of type **5** follow the same SAR rules as the 5-dipropylamino-4,5,6,7-tetrahydropyrazolo[1,5-*a*]pyridines (**4**), chlorination and formylation in position 3 were intended. Thus, treatment of **5a** with *N*-chlorosuccinimide in refluxing chloroform afforded the 3-chloro derivative **5b** in 69% yield. Employing Vilsmeier reaction conditions, the tetrahydropyrazolopyridine **5a** was transformed into the fused pyrazole carbaldehyde **5c** (Scheme 2).

For the preparation of the tricyclic ergoline analogue **6**, we recently established a multistep reaction sequence involving a Dieckmann type condensation and an electrophilic amination as the key reaction steps. For the development of a more practical approach, we envisioned taking advantage of the heterocyclic building block **13**, which we currently used for the synthesis and SAR studies of selective dopamine D_4 receptor ligands (Scheme 3).[24] Knoevenagel type condensation reaction of the carbaldehyde **13** with nitromethane gave the nitroolefin **14**. Subsequent sodium borohydride promoted reduction of the C═C double bond resulted in formation of the saturated synthetic intermediate in 82% yield. As the key reaction step, phosphorus oxychloride promoted Vilsmeier formylation followed by cyclocondensation afforded the periannelated system **15** in 51% yield. Consecutive reductions of C═C double bond and the nitro group using sodium borohydride and tin powder afforded the primary amine **16**. Finally, reductive N-propylation and sodium triacetoxyborohydride promoted N-alkylation with 4,4-phenylbenzoylaminobutylcarbaldehyde gave rise to the final product **7**.

Ligand Binding. To evaluate the biological impact of an arenecarboxamide derived molecular appendage, radioligand displacement assays were done. The binding affinity and selectivity profiles of target compounds of types **5** and **7** were compared with those of the core structure **4** and the phenylpiperazine derived reference agent **2** (Table 1). The binding data were generated by measuring the ability of the test compounds to compete with [^{3}H]spiperone for the cloned human dopamine receptor subtypes D_{2long}, D_{2short}, D_3, and $D_{4.4}$ stably expressed in Chinese hamster ovary (CHO) cells. D_1 receptor affinities were determined utilizing porcine striatal membranes and the D_1 selective radioligand [^{3}H]SCH 23390. Our initial investigations evaluated binding properties associated with the fused pyrazole **5a** as our primary target molecule. The biphenylcarboxamide derived molecular appendage, formally ligated to one of the *N*-propyl groups of the lead compound **4**, led to a substantial increase of D_3 affinity (racemic **5a**, K_i = 0.71 nM,). Binding affinity for the subtypes D_{2long}, D_{2short}, and D_4 increased only moderately (K_i of 150, 77, and 59 nM, respectively) compared to that of dipropylamine **4**. Comparison of the binding affinities indicates that the formal elongation of the propyl chain leads to an increase of D_3 receptor selectivity, which proved to be greater than 2 orders of magnitude. In accordance with our recent observations on the dipropylamines of type **4**,[19] the introduction of a chlorine substituent into position 3 of the heterocyclic system did not significantly affect the ligand binding properties (K_i = 0.59 for **5b**). In contrast, the attachment of a formyl group led to an approximately 50-fold attenuation of receptor recognition for the carbaldehyde **5c**. These data indicated that compounds of types **4** and **5** might interact with the D_3 receptor binding site in a similar mode. The tricyclic pyrazole derivative **7** revealed highly potent and selective D_3 receptor binding with selectivity patterns that were similar to that of the bicyclic congener of type **5**. Only poor to moderate D_1 and α_1 receptor affinity was observed for the test compounds. This was in contrast to the phenylpiperazine derived reference agent **2** showing a K_i of 5.6 nM for the α_1 adrenoreceptor (Table 1).

Because D_2, D_3, and D_4 receptors showed substantial differentiation between the two enantiomers of the dipropylamine **4** with ratios of >70, we investigated detailed binding properties of the optical antipodes (*R*)-**5a** and (*S*)-**5a**. Determination of binding affinity to the high affinity state of D_{2long} and D_3 receptors facilitates an adequate measurement of subtype selectivity.[25] Therefore, we performed displacement experiments with (*S*)-**4**, (*S*)-**5a**, and (*R*)-**5a** at the high affinity binding site of the D_{2long} and D_3 receptor which was selectively labeled with the agonist radioligand [^{3}H]7-OH-DPAT. The radioligand displacement assays were performed in a sodium free buffer supplemented with $MgCl_2$ (5 mM). At the D_3 receptor, K_i values were 14,

Table 1. Receptor Binding Data for 2, 4, 5a−c, and 7 Employing Porcine D_1 Receptor, the Human Subtypes D_{2long}, D_{2short}, D_3, and $D_{4.4}$ and the Porcine α_1 Receptor

	$K_i \pm$ SEM (nM)[a]					
		[^{3}H]spiperone				
compd	[^{3}H]SCH 23390 pD_1	hD_{2long}	hD_{2short}	hD_3	$hD_{4.4}$	[^{3}H]prazosin $p\alpha_1$
2	570 ± 26	48 ± 6.8	42 ± 2.4	0.22 ± 0.010	27 ± 4.4	5.6 ± 0.84
(*S*)-**4**	53000 ± 17000[b]	410 ± 88	270 ± 51	31 ± 4.8	380 ± 21	5100 ± 920[b]
(*R*)-**4**	68000 ± 11000[b]	55000 ± 13000	53000 ± 15000	2100 ± 370	17000 ± 4700	2900 ± 470[b]
5a	6800 ± 430	150 ± 14	77 ± 25	0.71 ± 0.076	59 ± 9.9	520 ± 2.5
5b	3600 ± 450	100 ± 15	43 ± 11	0.59 ± 0.088	190 ± 36	260 ± 26
5c	23000 ± 5300	8400 ± 2300	4700 ± 950	39 ± 6.9	6300 ± 840	3800 ± 1900
7	1800 ± 210	270 ± 42	240 ± 89	0.55 ± 0.10	230 ± 60	86 ± 5.5

[a] $K_i \pm$ standard error of mean derived from three to nine experiments each done in triplicate. [b] $K_i \pm$ standard deviation derived from two individual experiments each done in triplicate.

dx.doi.org/10.1021/jm101639t |*J. Med. Chem.* 2011, 54, 2477–2491

Table 2. Characterization of the High Affinity Binding Site for (*S*)-4, (*R*)-4, (*S*)-5a, and (*R*)-5a Employing the Human Subtypes D_{2long} and D_3 Receptor

		$K_i \pm$ SEM (nM)[a]			
receptor		(*S*)-4	(*R*)-4	(*S*)-5a	(*R*)-5a
D_{2long}	[^{3}H]spiperone	410 ± 88	55000 ± 13000	5.3 ± 0.55	300 ± 42
	Hill Slope (n_H)	−0.51 ± 0.018	−0.90 ± 0.067	−0.51 ± 0.006	−0.65 ± 0.075
	[^{3}H]7-OH-DPAT	4.6 ± 0.65[b]	57000 ± 34000[b]	1.0 ± 0.24	49 ± 12[b]
D_3	[^{3}H]spiperone	31 ± 4.8	2100 ± 370	0.19 ± 0.024	15 ± 3.8
	Hill Slope (n_H)	−0.93 ± 0.10	−0.84 ± 0.079	−0.81 ± 0.033	−0.84 ± 0.049
	[^{3}H]7-OH-DPAT	14 ± 4.3	4300 ± 1800[b]	0.027 ± 0.0044	6.3 ± 1.2

[a] $K_i \pm$ standard error of mean derived from three to eight experiments each done in triplicate. [b] $K_i \pm$ standard deviation derived from two individual experiments each done in triplicate.

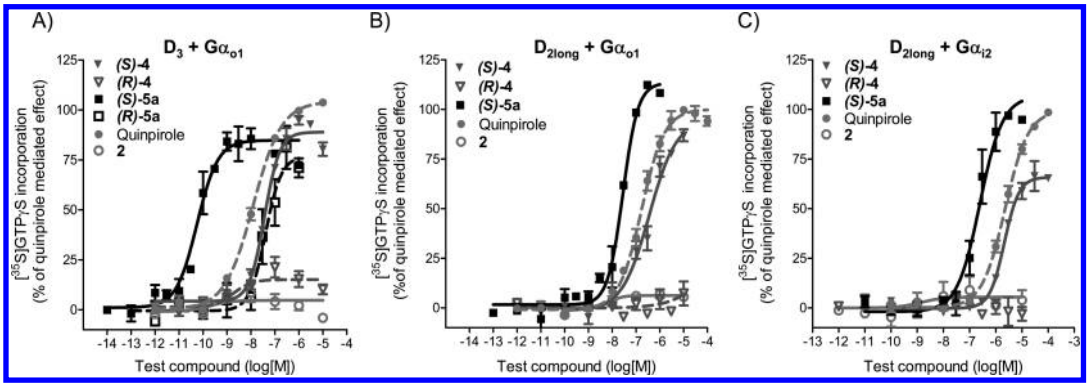

Figure 1. D_{2long} and D_3 receptor mediated [^{35}S]GTPγS incorporation in the presence of PTX-insensitive Gα_{o1} or Gα_{i2} subunits as a matter of receptor activation. The assay was performed on membrane preparations of transiently transfected HEK cells expressing given dopamine receptor and G$_\alpha$ protein. Normalized curves from three to six experiments, each performed in eight replicates, are shown. The error bars represent the SEM.

0.027, and 6.3 nM for **(*S*)-4**, **(*S*)-5a**, and **(*R*)-5a**, respectively. An exchange of one propyl unit of **(*S*)-4** (K_i = 14 nM) by the carboxamidobutyl function of **(*S*)-5a** caused a 520-fold increase of binding with an outstanding K_i of 0.027 nM (Table 2). At the D_{2long} receptor, K_i values were 4.6, 1.0, and 49 nM for **(*S*)-4**, **(*S*)-5a**, and **(*R*)-5a**, respectively. By employment of these values to determine subtype selectivity, the reference dipropylamine **4** preferentially recognized D_2 (3-fold). In contrast, the long chain derivatives **(*S*)-5a** and **(*R*)-5a** showed a 37- and 8-fold D_3 selectivity over D_{2long} receptor. Eudismic ratios of 49 and 230 were calculated for the subtypes D_{2long} and D_3, respectively, indicating that the receptor ligand interactions of **5a** strongly depend on the absolute stereochemistry of the enantiomers.

Functional Characterization. To investigate the impact of structural hybridization on the activity profiles of our newly synthesized compounds at the D_{2long} and D_3 receptors, we measured the [^{35}S]GTPγS incorporation in the presence of different pertussis toxin (PTX) insensitive Gα subunits, the inhibition of adenylyl cyclase, and the stimulation of [^{3}H]thymidine incorporation. We also investigated the influence of our test compounds on dopamine receptor internalization in a biotin protection assay and in antibody-feeding experiments.

Preferential coupling of the D_{2long} receptor with Gα_{o1} and Gα_{i2} subunits has been described.[26,27] Thus, we intended to measure D_{2long} receptor mediated incorporation of [^{35}S]GTPγS in the presence of PTX-insensitive Gα_{o1} or Gα_{i2} subunits. By use of this system, the reference compound **2** behaved as an antagonist. In contrast, our dopaminergic test compound **(*S*)-5a** displayed substantial ligand efficacy. The EC_{50} values of **(*S*)-5a** were 26 and 370 nM at the D_{2long}/Gα_{o1} and D_{2long}/Gα_{i2} membrane preparations, respectively (Figure 1B and Figure 1C). Despite significant absolute difference in the EC_{50} values between assays performed on the D_{2long}/Gα_{o1} and D_{2long}/Gα_{i2} membrane preparations, a comparison relative to the reference quinpirole indicated that **(*S*)-5a** behaved similarly in both assays. To put this observation in terms of numbers, the operational model of agonism[28] was applied to quantify the relative ability of a ligand to produce a response in a given system. We used this model previously to analyze ligand biased signaling at the D_{2long} receptor.[29] The operational model of agonism enables the description and quantification of agonist bias for a selected signaling pathway in terms of affinity and efficacy.[30,31] In this model, the affinity (K_A) describes an equilibrium dissociation constant of an agonist−receptor complex and the transduction coefficient (τ) is a parameter encompassing both the efficacy of an agonist and the sensitivity of a system. The value of $\Delta \log(\tau/K_A)$ relative to a chosen standard (e.g., full agonist like quinpirole) for a system is calculated to quantify the relative ability of each agonist to produce a response. The difference of the $\Delta \log(\tau/K_A)$ between selected pathways yields $\Delta\Delta \log(\tau/K_A)$, which describes agonist bias or functional selectivity of a given ligand. The quantification of relative ability of **(*S*)-5a** to produce agonistic response ($\Delta \log(\tau/K_A)$, relative to quinpirole) gave values of 11 and 17 at D_{2long}/Gα_{o1} and D_{2long}/Gα_{i2} membrane preparations, respectively (Supporting Information). These comparable $\Delta \log(\tau/K_A)$ values implied that **(*S*)-5a** is not functionally selective between Gα_{o1} or Gα_{i2}. Functional

dx.doi.org/10.1021/jm101639t |*J. Med. Chem.* 2011, 54, 2477–2491

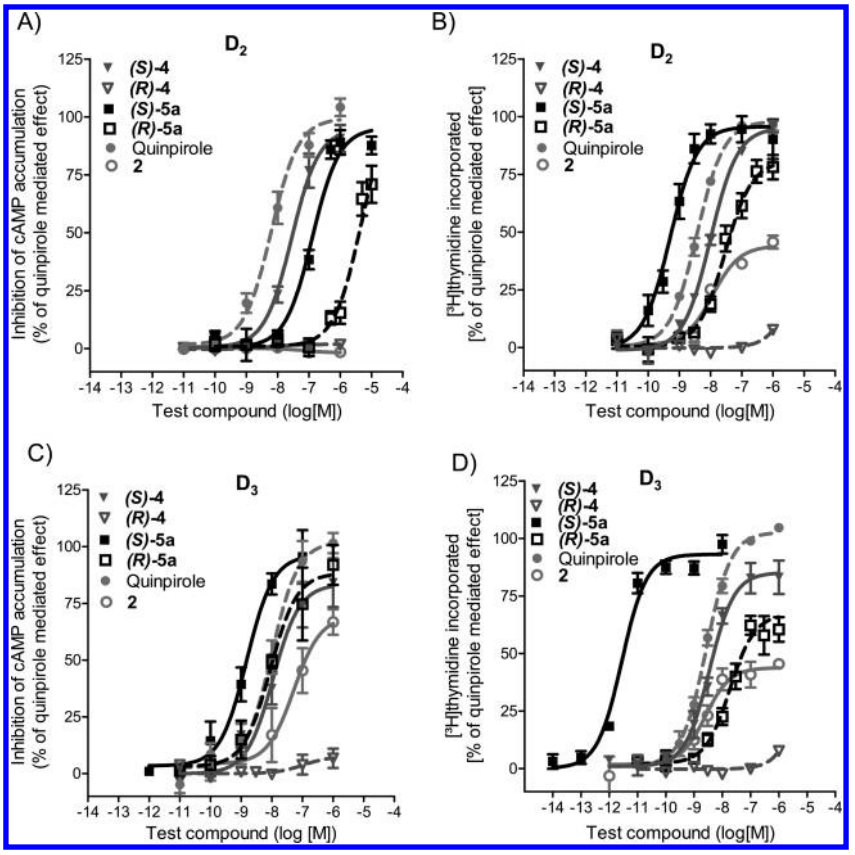

Figure 2. Intrinsic activity of the compounds **2**, (*S*)-**4**, (*S*)-**5a**, and (*R*)-**5a** at the D_{2long} and D_3 receptors measured by inhibition of cAMP accumulation and stimulation of [^{3}H]thymidine incorporation (mitogenesis assay). Both assays were performed on whole CHO cells, stably expressing given dopamine receptor. The cAMP production was stimulated with 20 μM forskolin (the D_{2long} receptor) and 2 μM forskolin (the D_3 receptor). Normalized curves from three to six experiments, each performed in triplicate, are shown. The error bars represent the SEM.

selectivity at the level of Gα subunits coupling was reported for propylnorapomophine (NPA), dinapsoline, and *S*-(3)-PPP.[32,33]

Because D_3 couples almost exclusively with the $G\alpha_{o1}$ subunit,[26] [^{35}S]GTPγS incorporation was measured in the presence of a coexpressed PTX-insensitive $G\alpha_{o1}$ subunit. Thereby, the reference compound **2** behaved as an antagonist (Figure 1A) while formal exchange of the phenylpiperazine moiety by the heterocyclic dipropylamine of type **4** yielded the superpotent agonist (*S*)-**5a** with an EC_{50} of 0.056 nM . The optical antipode (*R*)-**5a** behaved also as a full agonist but with 910-fold reduced potency (EC_{50} = 51 nM).

To further characterize the functional properties of our highly potent agonist (*S*)-**5a**, D_{2long} and D_3 receptor mediated inhibition of cAMP accumulation and the stimulation of [^{3}H]-thymidine incorporation were measured in CHO cells expressing the corresponding receptor. For the D_3 receptor, we reported that coupling of enyne units with *N*-butyl-4-biphenylcarboxamides resulted in a significantly biased functional outcome.[16] The enyne unit alone did not demonstrate any functional selectivity between the selected pathways. When coupled with *N*-butyl-4-biphenylcarboxamide, a strong ligand bias was observed. This long chain compound strongly preferred the D_3 receptor mediated stimulation of [^{3}H]thymidine incorporation, where it behaved as a full agonist. Simultaneously it behaved only as weak partial agonists in the inhibition of adenylyl cyclase.[16] For the D_{2long} receptor, we reported very recently that subtle modifications of the phenylpiperazine moiety significantly modulate ligand biased signaling (functional selectivity).[29] Here, the reference compound **2** induced significant ligand biased signaling at the D_{2long} receptor, behaving as an antagonist in the inhibition of cAMP accumulation and as a partial agonist (EC_{50} = 12 nM) in the stimulation of [^{3}H]thymidine incorporation (Figure 2A, Figure 2B). This is in accordance with our previous work, where we described the phenylpiperazine **2** as a functionally selective ligand, strictly preferring the ERK1/2 pathway over cAMP signaling.[29] The test compounds (*S*)-**4** and (*R*)-**5a** were full agonists in both pathways investigated but with a decreased potency compared with quinpirole (Figure 2A, Figure 2B). The use of operational model of agonism demonstrated that (*S*)-**4** does not exhibit any ligand bias. Compound (*R*)-**5a** showed some ligand bias ($\Delta\Delta\log(\tau/K_A)$), preferring the stimulation of [^{3}H]thymidine incorporation 80-fold over the inhibition of cAMP accumulation. The ability of the full agonist (*S*)-**5a** to inhibit cAMP accumulation (EC_{50} = 110 nM, Figure 2A) was weaker than that of quinpirole, whereas its ability to stimulate [^{3}H]thymidine incorporation (EC_{50} = 0.51 nM) was greater than that of the reference. According to the operational model of agonism, biased signaling of (*S*)-**5a** resulted in a 170-fold preference for the stimulation of [^{3}H]thymidine incorporation over the inhibition of cAMP accumulation.

At the D_3 receptor with the exception of (*S*)-**5a** all compounds displayed weaker agonist properties than quinpirole ($\Delta\log(\tau/K_A)$ values negative) and no substantial ligand biased signaling could be observed (Figure 2C and Figure 2D). Compared to quinpirole for compound (*S*)-**5a** a 7-fold better agonism was indicated in its ability to inhibit cAMP accumulation (Figure 2B).

dx.doi.org/10.1021/jm101639t |*J. Med. Chem.* 2011, 54, 2477–2491

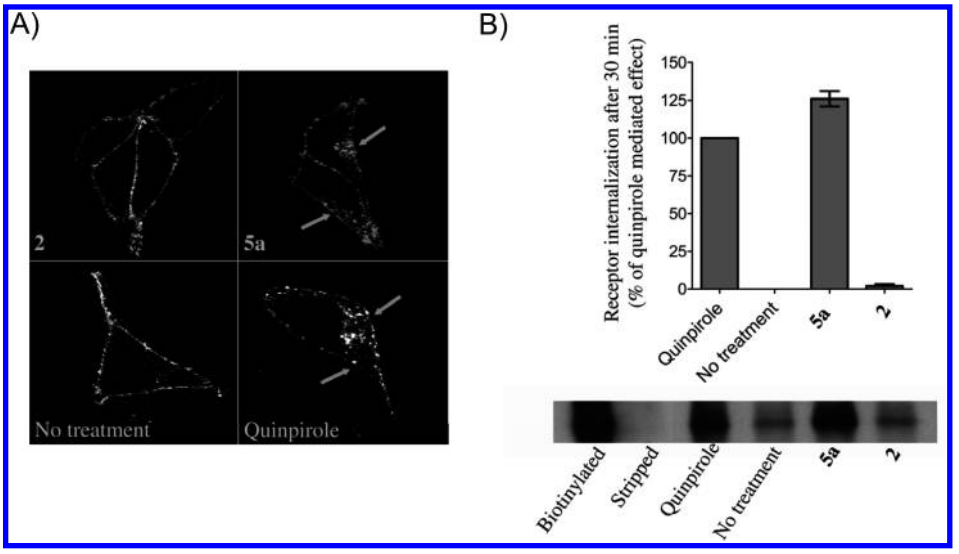

Figure 3. Ligand induced D_{2long} receptor internalization. (A) FLAG-tagged D_{2long} receptors expressed stably in HEK293 cells were incubated with M1 antibody followed by treatment with 10 μM **2** (upper panel, left), 10 μM **5a** (upper panel, right), 10 μM quinpirole (lower panel, right) or left untreated (lower panel, left). Treatment with quinpirole or **5a** potently induced D_{2long} receptor internalization (indicated with arrows). No internalization was observed after incubation with **2**. (B) HEK 293 cells stably expressing the FLAG-tagged D_{2long} receptor were surface biotinylated (lane 1) and then stripped (lane 2), incubated with 10 μM quinpirole (lane 3), left untreated (lane 4), incubated with 10 μM **5a** (lane 5) or with **2** for 30 min (lane 6). The bar chart represents the mean recovery of surface biotinylated receptors (relative to 30 min of stimulation with 10 μM quinpirole).

Because of the fact that (*S*)-**5a** stimulated [^{3}H]thymidine incorporation (EC_{50} = 0.0028 nM) with a 820-fold greater potency than quinpirole (Figure 2D), this yields about 140-fold functional selectivity of (*S*)-**5a** for the stimulation of [^{3}H]thymidine incorporation over the inhibition of cAMP accumulation according to the operational model. One of the most potent reported D_3 receptor agonist (*S*)-*N*-(4-((2-amino-4,5,6,7-tetrahydrobenzo[*d*]thiazol-6-yl)(propyl)amino)butyl)-2-naphthamide with a modest D_2/D_3 selectivity and a binding affinity of 0.043 nM on the D_3 receptor was unfortunately tested only in a mouse model, making the comparison of functional data not possible.[34]

To investigate the ability of racemic **5a** to promote D_{2long} receptor endocytosis, antibody feeding experiments were performed. Therefore, live cells expressing the extracellular FLAG-tag D_{2long} receptor were incubated with the M1 antibody directed against the FLAG epitope to label the mature pool of receptors at the plasma membrane.[35] Cells were then left untreated or treated with quinpirole (positive control), **2** or **5a** at 10 μM, because in a typical antibody feeding experiment, cells are stimulated with saturating concentrations of compounds.[35,36] Both quinpirole and **5a** induce receptor internalization indicated by translocation of the receptor from the plasma membrane to the cytosol (Figure 3A). To quantify the internalization rate of the D_{2long} receptor after stimulation with the different ligands, a biotin protection/degradation assay, which measures internalization of biotinylated receptors by inaccessibility to a membrane impermeable reducing agent, was used. No internalization for the phenylpiperazine **2** but a significant endocytosis in response to quinpirole and **5a** could be observed, which is in good agreement with the results of the antibody feeding experiment. By use of this quantitative assay, it is possible to conclude that the internalized receptor pool for quinpirole is similar to that of **5a** (Figure 3B). In contrast to the D_{2long} receptor, the D_3 subtype does not undergo agonist-mediated internalization.[36,37] In accordance with these reports, we have not observed any change in the receptor distribution upon the stimulation of the D_3 receptor with agonists quinpirole and **5a**.

Mutagenesis of the D_3 Receptor. Our previous SAR studies on phenylpiperazines combining chemical synthesis, molecular modeling, and site-directed mutagenesis demonstrated that Asp3.32 and discrete amino acids interacting with the dopamine simulating headgroup (e.g., Ser5.42, Ser5.46, Phe6.51, Phe6.52, and His6.55) and with an affinity generating lipophilic appendage (e.g., Val2.61, Leu2.64, Phe3.28, and Val3.29) importantly modulate the binding of phenylpiperazines.[38] These residues also serve for the intermolecular recognition of the antagonist eticlopride as evident from the D_3 receptor crystal structure.[20]

To investigate if the tetrahydropyrazolopyridines of types **4** and **5** utilize the same contacting amino acids as the phenylpiperazine **2**, diagnostic residues were mutated to determine their influence on binding affinity. The residue Asp3.32, which interacts with the ligands' cationic ammonium center,[16,20,38] was mutated to glutamate.[38] The affinity of (*S*)-**5a** dropped drastically (11000-fold) underscoring the important contribution of Asp3.32 to the binding affinity of the extremely well aligned ligand (Table 3). The affinity of the compounds (*S*)-**4** and (*R*)-**5a** with poorer starting affinities was reduced only up to 74-fold.

The conserved serines Ser5.42, Ser5.43, and Ser5.46 in TM5 represent an important dopamine receptor microdomain that is involved in the hydrogen bonding with the catechol hydroxyl groups of dopamine.[39−41] Ser5.42 was described as the important residue in the D_3 receptor for the interaction with dopamine-like agonists.[39] As evident from the crystal structure, Ser5.42 interacts with the antagonist eticlopride.[20] While the affinities of (*S*)-**5a**, (*S*)-**4**, and (*R*)-**5a** were attenuated 30-fold, 5.6-fold, and 13-fold, respectively, for Ser5.42, the mutation Ser5.46Ala had no significant influence on the affinity of the compounds. This was expected because our test compounds exhibit only one polar function in their headgroups, which is obviously tied up in an interaction with Ser5.42. The mutation His6.55Ala led to an increase in affinity of the 1,4-disubstituted phenypiperazine **2**,

Table 3. Binding Data of Compounds 2, (*S*)-4, (*S*)-5a, and (*R*)-5a at the D_3 Wild Type and Mutant Receptors

	$K_i \pm$ SEM (nM)[a]			
receptor	**2**	(*S*)-**4**	(*S*)-**5a**	(*R*)-**5a**
D_3wt	0.90 ± 0.22	150 ± 30	0.076 ± 0.0059	19 ± 3.8
D_3D3.32E	790 ± 81 (880)	8100 ± 2000 (54)	850 ± 280 (11000)	1400 ± 760 (74)
D_3V2.61F	180 ± 5.0 (200)	420 ± 78 (2.8)	170 ± 17 (2200)	3700 ± 1100 (190)
D_3S5.42A	2.8 ± 0.30 (3.1)	840 ± 100 (5.6)	2.3 ± 0.52 (30)	240 ± 80 (13)
D_3S5.46A	0.16 ± 0.010 (0.18)	45 ± 6.0 (0.30)	0.058 ± 0.0059 (0.76)	15 ± 0.58 (0.79)
D_3H6.55A	0.58 ± 0.060 (0.64)	420 ± 73 (2.8)	0.98 ± 0.079 (12)	43 ± 6.7 (2.3)

[a] Data derived from competition binding experiments with [^{3}H]spiperone at D_3 wild type and mutant receptors transiently expressed in HEK 293 cells. Values are given as mean $K_i \pm$ SEM of 3−12 independent experiments each done in triplicate. Fold changes in affinity compared to wild type are indicated in parentheses.

which was more distinct for our previously characterized phenylpiperazines.[38] On the other hand the affinities of the dipropylamine (*S*)-**4** and its derivatives (*S*)-**5a** and (*R*)-**5a** decreased at the His6.55Ala receptor (3-, 12-, and 2-fold, respectively). The activation of 7TM receptors encompasses a movement of transmembrane helices in particular of TM6 in a rigid-body fashion making vertical "see-saw" movement toward TM3 and resulting in a closing around the main ligand-binding pocket at the extracellular side and an opening at the intracellular side for G-protein binding.[42−45] We speculate that during the activation and the transition of the receptor into the high affinity state (coupled with trimeric G-proteins) agonists favorably interact with His6.55 whereas repulsive interactions perturb conformational changes of antagonist bound complexes. Apparently, the mutation His6.55Ala nullifies beneficial interactions between His6.55 and the agonists of types **4** and **5** that take place during receptor activation.

To observe binding interactions of the ligands' lipophilic appendages, Val2.61 was mutated by the more sterically demanding phenylalanine.[20,38,46−48] The mutation Val2.61Phe substantially attenuated ligand binding of the long chain derivatives **2**, (*S*)-**5**, and (*R*)-**5** leading to a 200-, 2200-, and 190-fold reduction of affinity, respectively. On the other hand, D_3 recognition of the dipropylamine (*S*)-**4** was only slightly influenced. These data indicate that the introduction of the sterically more demanding phenylalanine at position 2.61 hinders the binding of long chain ligands at the D_3 receptor, thus restricting the optimal length of synthetic ligands and contributing to $D_2/D_3/D_4$ selectivity. The identification of a critical ligand length that induces a clash with the mutation Val2.61Phe will give valuable insights into the determinants for D_2, D_3, D_4 subtype selectivity and thus for a rational drug design.

Ligand Docking and Analysis. To better understand the binding modes of our test compounds and the results of the mutagenesis experiments at the D_3 receptor, ligand docking and a careful analysis of the obtained complexes were performed. The tetrahydropyrazolopyridines (*R*)-**5a** and (*S*)-**5a** and the reference phenylpiperazine **2** were docked into the crystal structure of the recently published dopamine D_3 receptor by means of AUTODOCK4.[20,49−51] Ligands were subjected in protonated form at the basic amine to enable the formation of the essential charge reinforced hydrogen bond between ligand and Asp3.32 in TM3. The protonation of the tertiary amine of (*R*)-**5a** and (*S*)-**5a** resulted in two diastereoisomers, which bound differently to the D_3 receptor structure with respect of the orientation of the propyl moiety. The (*R*)-N isomer of (*R*)-**5a** and (*S*)-**5a** formed a receptor−ligand complex in which the propyl group points toward TM7 enclosed by Asp3.32, Trp6.48, and Thr7.39. In contrast, the propyl moiety of the (*S*)-N isomer was positioned close to TM3 surrounded by Leu3.29, Asp3.32, and Val3.33. According to earlier studies on the binding mode of dopamine receptor agonists, the propyl moiety binds to a "propyl cleft" that extends from Asp3.32 of TM3 toward TM2 and TM7.[52] Only the (*R*)-N isomer of (*R*)-**5a** and (*S*)-**5a** possesses the possibility to occupy this microdomain and was therefore chosen for further analysis.

Docking of the phenylpiperazine **2** resulted in docking poses that were similar to receptor−ligand complexes of related phenylpiperazine derivatives.[38] On the basis of DrugScore[online] scoring values[53] and experimental data, a final complex was selected and subjected to energy minimization. Docking of (*R*)-**5a** and (*S*)-**5a** resulted in two ligand−receptor complexes in each case, which showed a distinct position and orientation of the tetrahydropyrazolopyridine moiety. All four complexes were submitted to energy minimization. On the basis of a careful analysis of the complexes and recent D_3 mutagenesis data, the receptor−ligand complexes presented in Figure 4 were chosen for further investigations. Conserved serine residues located at positions 5.42, 5.43, and 5.46 in TM5 play an important role in the binding dopamine-like agonists and the dopamine receptor activation.[39−41] The side chain conformation of Ser5.42 enabled formation of a hydrogen bond with the lone pair of the tetrahydropyrazolopyridine moiety of (*R*)-**5a** and (*S*)-**5a**. In accordance with the crystal structure of the β_2-adrenergic receptor bound to the agonist FAUC 50,[54] the side chain of Ser5.43 was rearranged before energy minimization, yielding a conformation where it points into the binding pocket.

As expected from recent crystal structures, analysis of the final receptor−ligand complex models showed a polar interaction between Asp3.32 and the cationic ammonium group. The tetrahydropyrazolopyridine head groups of (*R*)-**5a** and (*S*)-**5a** (Figure 4B) formed hydrophobic interactions with the amino acids residues Val3.33, Ser5.46, Phe6.51, Phe6.52, and His6.55. An analogous binding mode was observed for the phenylpiperazine moiety of our reference compound **2** (Figure 4A); the methoxy group was located in proximity to His6.55. This is different for the tetrahydropyrazololpyridine headgroup of (*R*)-**5a** and (*S*)-**5a**, which is more distant to this residue. These results are in agreement with our mutagenesis data, when a higher susceptibility indicated differential binding properties of phenylpiperazines and (*R*)-**5a**/(*S*)-**5a**.[38] In the region of TM5 we observed that our reference compound **2** does not form hydrogen bonds to serine residues whereas the endocyclic nitrogen of the tetrahydropyrazolopyridine moiety of (*R*)-**5a** and (*S*)-**5a** forms a hydrogen bond interaction with Ser5.42, but not with

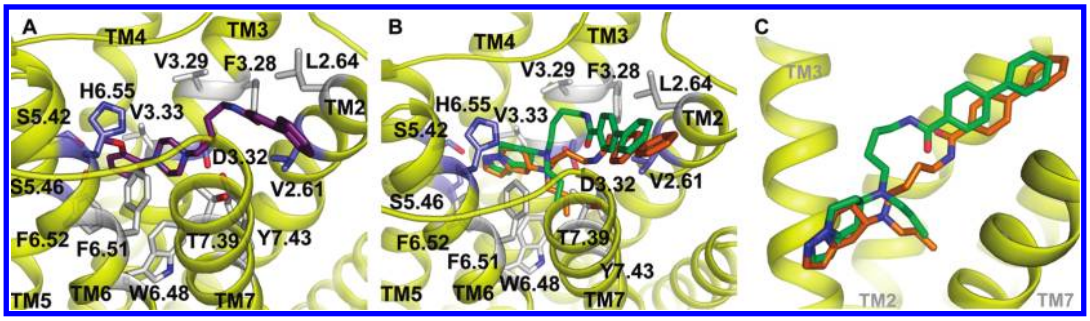

Figure 4. Reference ligand **2** (A) and test compounds (*R*)-**5a** and (*S*)-**5a** (B and C) docked into the crystal structure of the dopamine D3 receptor. Residues involved in ligand binding and the ligands are represented as sticks. The D3 receptor backbone is represented as yellow ribbons. **2** is indicated in violet. (*R*)-**5a** is colored in green, and (*S*)-**5a** is shown in orange. Residues involved in mutagenesis experiments are presented in blue.

Table 4. Influence of the Mutation Val2.61Phe in the D_3 Receptor on the Binding Affinity of the Ligands 17−21 Depending on the Size of Their Lipophilic Appendage

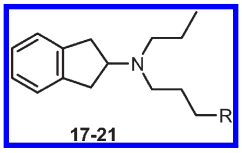

		$K_i \pm$ SEM (nM)[a]		
compd	R	D_3wt	D_3V2.61F	susceptibility[b] K_i^{mut}/K_i^{wt}
17	H	230 ± 87	350 ± 87	1.5
18	methylcarbonylaminomethyl	410 ± 65	330 ± 57	0.8
19	butylcarbonylaminomethyl	44 ± 11	760 ± 89	17
20	benzylcarbonylaminomethyl	2.7 ± 0.6	250 ± 40	93
21	biphenylcarbonylaminomethyl	1.0 ± 0.2	230 ± 48	230

[a] Binding data were determined in competition binding experiments with [^{3}H]spiperone at the D_3 wild type and the D_3 Val2.61Phe mutant receptors transiently expressed in HEK 293 cells. Values given are mean $K_i \pm$ SEM of three to eight independent experiments each done in triplicate; [b] Susceptibility of the mutation on ligand binding expressed by the ratio K_i^{mut}/K_i^{wt}, changes in affinity compared to wild type.

Ser5.43. These results were also supported by our mutagenesis experiments.

Receptor binding studies revealed a 250-fold better affinity of the eutomer (*S*)-**5a** to the D_3 receptor compared to the distomer (*R*)-**5a**. According to our mutagenesis experiments at D_3, Asp3.32Glu exchange led to a drastic decrease in affinity of (*S*)-**5a**, whereas (*R*)-**5a** reacted less sensitively to this mutation. The comparison of the docking poses (Figure 4C) showed that eutomer and distomer of **5a** differ in position and orientation of the ammonium center, the propyl moiety and the chain linking the biphenylcarboxamide moiety. Different binding energies resulting from the distinct orientations would explain the reduced D_3 affinity and decreased sensitivity of (*R*)-**5a** toward Asp3.32Glu D_3 mutation.

The *N*-butylbiphenylcarboxamide appendage of all three ligands is in proximity to a microdomain that consists of residues at position 2.61, 2.64, 3.28, and 3.29 at TM2 and TM3, which is known to be responsible for $D_2/D_3/D_4$ selectivity.[20,38,46−48]

To better understand these interactions, a series of compounds was synthesized and investigated, in which we gradually elongated the chain length, and was tested in the radioligand displacement assays using [^{3}H]spiperone. As a molecular probe to determine the critical length of ligands, the achiral aminoindane molecular scaffold was chosen. Aminoindane derivatives are easily accessible and were previously described as high affinity agonists for D_2-like receptors.[55,56] Starting from the 2-*N*,*N*-dipropylaminoindane[55] core structure (**17**), the length of the appendage was gradually increased to reach the size of the *N*-butylbiphenylcarboxamide substituted aminoindane[56] **21** as depicted in Table 4.

After characterization of the molecular probes **17**−**21** toward diagnostic D_3 mutants (Supporting Information) binding affinities of the 2-dipropylaminoindane **17** and its methyl (**18**), butyl (**19**), phenyl (**20**), and biphenyl (**21**) carboxamidomethyl substituted derivatives were tested at D_3 wild type compared to the Val2.61Phe mutant (Table 4). The mutation Val2.61Phe had no influence on the binding affinity of 2-dipropylaminoindane (**17**) and the methylcarboxamidomethyl substituted derivative **18**. Further elongation of the appendage by formal exchange of the methyl residue by a butyl group at the carboxamide caused significant susceptibility of the test compound **19** toward the Val2.61Phe mutation, resulting in a 17-fold reduction of binding affinity. Evaluation of the benzamide **20** indicated that a sterically more demanding phenyl substituent exerts substantial repulsion with the phenylalanine residue in position 2.61, leading to an almost 100-fold increase of the K_i. Finally, the biphenylcarboxamide **21** also displayed strongly impaired binding (230-fold reduction) that was comparable to the susceptibility of the biphenylcarboxamides of type **2** and **5**. Overall, however, the major interactions between our long chain ligands and the amino acid residue in position 2.61 of the D_3 receptor appear to originate in the substituent that is directly bound to the CO group of the aminocarbonyl function.

CONCLUSIONS

To learn more about the structural origins of the differential activity profiles, we could show that a formal structural hybridization of dopaminergic dipropylamines of type **1** with lipophilic appendages leads to novel dopaminergic chemotypes of types **5** and **7**. The biphenylcarboxamide (*S*)-**5a** displayed an outstanding K_i of 27 pM at the agonist-labeled D_3 receptor and significant selectivity over the D_2 subtype. Measurement of [^{35}S]GTPγS incorporation in the presence of a coexpressed PTX-insensitive Gα_{o1} subunit indicated highly efficient G-protein coupling. Comparison of ligand efficacy data from cAMP accumulation and [^{3}H]thymidine incorporation experiments revealed that the test compound (*S*)-**5a** displays ligand biased signaling with a

significant preference for [^{3}H]thymidine incorporation. This is in accordance to our recent observations with enyne-derived dopaminergics.[16]

Starting from the D_3 crystal structure,[20] a combination of homology modeling and site directed mutagenesis gave valuable insights into the binding mode and the intermolecular origins of stereospecific receptor recognition. The concept of biased ligands and functional selectivity at the 7TM receptors raises the possibility of developing chemical probes and drugs with precisely defined properties.[57] Mutagenesis data indicate that the eutomer can better take advantage from the charge-enforced hydrogen bond with the carboxylate function of Asp3.32. Thus, the favorable binding energy that results from the interaction between the ligand's central ammonium unit and the aspartate residue in position 3.32 obviously controls stereospecificity of binding.

Recent progress in the structural biology of the 7TM receptors provided important clues about the agonist-bound states of the β2 receptor.[54,58,59] The crystal structure of the 7TM receptor cocrystallized with both enantiomers of a very potent agonist like **5a** could provide most desirable structural information about the stereospecificity of binding.

EXPERIMENTAL SECTION

Chemistry. All reactions were carried out under nitrogen atmosphere. Dry solvents and reagents were commercial quality and used as purchased. MS were run on a Finnigan MAT TSQ 700 spectrometer by EI (70 eV) with solid inlet or with an ion-trap mass with APCI ionization. HR-EIMS were run on a Finnigan MAT 8200 using peak Peak-Matching ($M/\Delta M$ = 10000). NMR spectra were obtained on a Bruker Avance 360 or a Bruker Avance 600 spectrometer relative to TMS in the solvents indicated (J in Hz). IR spectra were performed on a Jasco FT/IR 410 spectrometer using a film of substance on a NaCl pill. Purification by flash chromatography was performed using silica gel 60 if not stated otherwise. TLC analyses were performed using Merck 60 F254 aluminum sheets and analyzed by UV light (254 nm) or by spraying with ninhydrin reagent. Analytical HPLC/MS was performed on Agilent 1100 HPLC systems employing a VWL detector connected to a Bruker Esquire 2000. A Zorbax SB-C18 (4.6 mm i.d. × 150 mm, 5 μm) was used as the column and run with a flow rate of 0.5 mL/min (eluent methanol/water/0.1 N formic acid, 10% methanol for 3 min to 100% methanol in 15 min, 100% for 6 min to 10% in 3 min, 10% for 3 min). CHN elementary analyses were performed at the Chair of Organic Chemistry, Friedrich Alexander University Erlangen-Nürnberg. HPLC was run with MeOH (eluent I) and 0.1% aqueous formic acid (eluent II) and the following gradient: MeOH 10% for 3 min ascending to 100% in 15 min, 100% for 6 min. Flow rate was 0.5 mL/min, and λ = 254 nm. All SAR compounds were determined to be >95% pure.

***N*-(4-(4-Phenylbenzoylamino)butyl)-*N*-propyl-5-amino-4,5,6,7-tetrahydropyrazolo[1,5-*a*]pyridine (5a), (*R*)-*N*-(4-(4-Phenylbenzoylamino)butyl)-*N*-propyl-5-amino-4,5,6,7-tetrahydropyrazolo[1,5-*a*]pyridine ((*R*)-5a), and (*S*)-*N*-(4-(4-Phenylbenzoylamino)butyl)-*N*-propyl-5-amino-4,5,6,7-tetrahydropyrazolo[1,5-*a*]pyridine ((*S*)-5a).** To a solution of **10**, (*R*)-**10**, or (*S*)-**10** (17 mg, 0.095 mmol) in 1,2-dichlorethane (2 mL) was added 4-(4-phenylbenzoylamino)butyraldehyde[23] (25 mg, 0.095 mmol) and sodium triacetoxyborohydride (30 mg, 0.14 mmol). The solution was stirred at room temperature for 18 h and extracted with saturated $NaHCO_3$. The organic layer was dried ($MgSO_4$) and evaporated, and the residue was purified by flash chromatography to give pure **5a**, (*R*)-**5a**, or (*S*)-**5a**, respectively (35 mg, 85%), as a colorless oil. Alternatively, enantiopure (*R*)-**5a** and (*S*)-**5a** could be obtained by chiral resolution of racemic **5a** employing HPLC separation with a Chiralcel OD column (Dycel, Hadleigh, U.K.) at a flow of 0.5 mL/min of isopropanol/hexane 1/1: t_R = 22.8 min for (*R*)-**5a** and t_R = 20.6 min for (*S*)-**5a**. IR: 3320, 2950, 2930, 1640, 1550, 1490, 1300, 700 cm^{-1}. ^{1}H NMR ($CDCl_3$, 360 MHz) δ 0.89 (t, J = 7.5 Hz, 3H), 1.41−1.72 (m, 6H), 1.92−2.04 (m, 1H), 2.11−2.17 (m, 1H), 2.47 (t, J = 7.5 Hz, 2H), 2.56 (t, J = 7.1 Hz, 2H), 2.68 (dd, J = 16.0, 11.0 Hz, 1H), 2.96 (dd, J = 16.0, 4.6 Hz, 1H), 3.05−3.13 (m, 1H), 3.47−3.53 (m, 2H), 4.04 (ddd, J = 12.7, 12.3, 4.9 Hz, 1H), 4.38 (ddd, J = 12.7, 5.6, 2.2 Hz, 1H), 5.96 (d, J = 1.8 Hz, 1H), 6.29 (br s, 1H), 7.36−7.49 (m, 4H), 7.59−7.67 (m, 4H,), 7.83 (br d, J = 8.5 Hz, 2H). EIMS m/z 430. Anal. ($C_{27}H_{34}N_4O$) C, H, N. (*R*)-**5a**: $[\alpha]_D^{20}$ 36.8° (c 0.5, $CHCl_3$). (*S*)-**5a**: $[\alpha]_D^{20}$ −36.3° (c 0.5, $CHCl_3$).

***N*-(4-(4-Phenylbenzoylamino)butyl)-*N*-propyl-5-amino-3-chloro-4,5,6,7-tetrahydropyrazolo[1,5-*a*]pyridine (5b).** To a solution of **5a** (16 mg, 0.037 mmol) in $CHCl_3$ (4 mL) was added *N*-chlorosuccinimide (10 mg, 0.075 mmol). The mixture was refluxed for 16 h, evaporated, and the residue was purified by flash chromatography (CH_2Cl_2/MeOH 95/5) to give **5b** (12 mg, 69%) as a colorless oil. IR: 3320, 2930, 1640, 1550, 1490, 1350, 1010, 750 cm^{-1}. ^{1}H NMR($CDCl_3$, 360 MHz) δ 0.89 (t, J = 7.3 Hz, 3H), 1.42−1.72 (m, 6H), 1.91−2.03 (m, 1H), 2.09−2.16 (m, 1H), 2.45−2.59 (m, 5H), 2.90 (dd, J = 16.3, 5.2 Hz, 1H), 3.05−3.13 (m, 1H), 3.48−3.53 (m, 2H), 4.01 (ddd, J = 12.7, 12.3, 4.6 Hz, 1H), 4.32 (ddd, J = 12.7, 5.4, 2.3 Hz, 1H), 6.25 (br s, 1H), 7.37 (s, 1H), 7.37−7.41 (m, 1H), 7.43−7.48 (m, 2H), 7.59−7.67 (m, 4H), 7.83 (br d, J = 8.6 Hz, 2H). MS m/z 464. Anal. ($C_{27}H_{33}ClN_4O$) C, H, N.

***N*-(4-(4-Phenylbenzoylamino)butyl)-*N*-propyl-5-amino-4,5,6,7-tetrahydropyrazolo[1,5-*a*]pyridine-3-carbaldehyde (5c).** To a solution of **5a** (20 mg, 0.047 mmol) in DMF (2 mL), $POCl_3$ (16 mg, 0.1 mmol) was added. The mixture was stirred at 90 °C for 2 h. Then H_2O and 2 N NaOH were added. The mixture was extracted with $CHCl_3$, and the organic layer was dried ($MgSO_4$) and evaporated. The residue was purified by flash chromatography (CH_2Cl_2/MeOH 97/3) to give **5c** (14 mg, 65%) as a colorless oil. IR: 3340, 2930, 1640, 1540, 1510, 1440, 1070, 750 cm^{-1}. ^{1}H NMR ($CDCl_3$, 360 MHz) δ 0.89 (t, J = 7.4 Hz, 3H), 1.42−1.72 (m, 6H), 1.97−2.09 (m, 1H), 2.15−2.20 (m, 1H), 2.48 (t, J = 7.4 Hz, 2H), 2.58 (t, J = 7.0 Hz, 2H), 2.89 (dd, J = 17.4, 10.3 Hz, 1H), 3.10−3.17 (m, 1H), 3.33 (dd, J = 17.4, 5.3 Hz, 1H), 3.47−3.53 (m, 2H), 4.10 (ddd, J = 13.3, 12.7, 5.4 Hz, 1H), 4.39 (ddd, J = 13.3, 5.3, 2.5 Hz, 1H), 6.25 (br s, 1H), 7.36−7.48 (m, 3H), 7.59−7.67 (m, 4H), 7.83 (br d, J = 8.4 Hz, 2H), 7.87 (s, 1H), 9.84 (s, 1H). MS m/z 458. Anal. ($C_{28}H_{34}N_4O$) C, H, N.

***N*-(4-(4-Phenylbenzoylamino)butyl)-*N*-propyl-4-amino-4,5-dihydro-3*H*-pyrazolo[4,5,1-*i,j*]quinoline (7).** (1) To a solution of **16** (40 mg, 0.23 mmol) in MeOH (5.5 mL) was added propionic aldehyde (135 mg, 2.32 mmol) and sodium cyanoborohydride (29 mg, 0.46 mmol). After the mixture was stirred for 45 min at 0 °C, aqueous HCl (1 N, 2 mL) and saturated $NaHCO_3$ (6 mL) were added. After addition of diethyl ether, the organic layer was dried ($MgSO_4$) and evaporated and the residue was purified by flash chromatography (CH_2Cl_2/MeOH 97/3) to give pure 4-propylamino-4,5-dihydro-3*H*-pyrazolo[4,5,1-*i,j*]quinoline (26 mg, 53%) as a colorless oil.[21]

(2) To a solution of 4-propylamino-4,5-dihydro-3*H*-pyrazolo[4,5,1-*i,j*]quinoline (20 mg, 0.093 mmol) in 1,2-dichloroethane (2 mL), 4-(4-phenylbenzoylamino)butyraldehyde[23] (25 mg, 0.093 mmol) and sodium triacetoxyborohydride (30 mg, 0.14 mmol) were added. The mixture was stirred at room temperature for 18 h. Then saturated $NaHCO_3$ and CH_2Cl_2 were added. The organic layer was dried ($MgSO_4$) and evaporated and the residue was purified by flash chromatography (CH_2Cl_2/MeOH 95/5) to give **7** (38 mg, 87%) as a colorless oil. IR: 3315, 2930, 1640, 1550, 1070, 750 cm^{-1}. ^{1}H NMR ($CDCl_3$, 360 MHz) δ 0.90 (t, J = 7.4 Hz, 3H), 1.43−1.75 (m, 6H), 2.54 (t, J = 7.3 Hz, 2H), 2.64 (t, J = 6.8 Hz, 2H), 2.79−3.02 (m, 4H), 3.21−3.30 (m, 1H), 3.48−3.53 (m, 2H), 6.32 (br s, 1H), 6.60 (dd, J = 6.8, 6.6 Hz, 1H), 6.67 (d, J = 6.6 Hz, 1H), 7.35−7.40 (m, 1H), 7.43−7.48 (m, 2H), 7.58−7.61 (m, 2H), 7.62 (br d, J = 8.4 Hz, 2H), 7.67 (s, 1H, H-2),

7.82 (br d, J = 8.4 Hz, 2H), 8.17 (d, J = 6.8 Hz, 1H). MS m/z 466. Anal. ($C_{30}H_{34}N_4O$) C, H, N.

5-Propylamino-4,5,6,7-tetrahydropyrazolo[1,5-*a*]pyridine (10), (*R*)-5-Propylamino-4,5,6,7-tetrahydropyrazolo[1,5-*a*]pyridine ((*R*)-10), and (*S*)-5-Propylamino-4,5,6,7-tetrahydropyrazolo[1,5-*a*]pyridine ((*S*)-10). A mixture of **9**, (*R*)-**9** or (*S*)-**9** (20 mg, 0.15 mmol), sodium cyanoborohydride (18.6 mg, 0.29 mmol), propionic aldehyde (106 μL, 1.5 mmol), and MeOH (4 mL) was stirred at 0 °C for 45 min. After addition of HCl (1 N, 3 mL) the mixture was basified with aqueous NaOH (2 N). After addition of diethyl ether the organic layer was dried ($MgSO_4$), evaporated and the residue was purified by flash chromatography (CH_2Cl_2/MeOH 9/1) to give pure **10**, (*R*)-**10** or (*S*)-**10** (17 mg, 65%), as a colorless oil. IR: 2960, 2920, 2780, 2730, 1440, 1320, 710 cm^{-1}. ^1H NMR ($CDCl_3$, 360 MHz) δ 0.87 (t, J = 7.4 Hz, 3H), 1.40−1.53 (m, 2H), 1.88−2.02 (m, 1H), 2.09−2.15 (m, 1H), 2.46 (t, J = 7.4 Hz, 2H), 2.65 (dd, J = 15.4, 11.0 Hz, 1H), 2.92 (dd, J = 15.4, 4.7 Hz, 1H), 3.01−3.15 (m, 1H), 4.02 (ddd, J = 12.9, 12.2 Hz, 4.5 Hz, 1H), 4.35 (ddd, J = 12.9, 5.6, 2.3 Hz, 1H), 5.96 (br d, J = 1.8 Hz, 1H), 7.42 (d, J = 1.8 Hz, 1H). MS m/z 179. Anal. ($C_{10}H_{17}N_3$) C, H, N. (*R*)-**9**: $[\alpha]_D^{20}$ 47.4° (*c* 0.5, $CHCl_3$). (*S*)-**9**: $[\alpha]_D^{20}$ −47.1° (*c* 0.5, $CHCl_3$).

4-(2-Nitrovinyl)pyrazolo[1,5-*a*]pyridine (14). To a mixture of **13** (590 mg, 4.0 mmol) in MeOH (6.5 mL) were added nitromethane (0.24 mL, 4.4 mmol), methylammonium chloride (100 mg), and potassium acetate (100 mg). The mixture was stirred for 3 days at room temperature. Then the precipitate was filtered and dried to leave pure **14** (610 mg, 80%) as a colorless solid (mp 162 °C). IR: 2360, 1640, 1510, 1330, 1190, 97 ss, 760 cm^{-1}. ^1H NMR ($CDCl_3$, 360 MHz) δ 6.74−6.75 (br d, J = 2.5 Hz, 1H), 6.72 (dd, J = 7.1, 7.1 Hz, 1H), 7.45 (d, J = 7.1 Hz, 1H), 7.76 (d, 13.8 Hz, 1H), 8.12 (d, J = 2.5 Hz, 1H), 8.16 (d, J = 13.8 Hz, 1H), 8.61−8.63 (br d, J = 7.1 Hz, 1H). MS m/z 189. Anal. ($C_9H_7N_3O_2$) C, H, N.

4-Nitro-5*H*-pyrazolo[4,5,1-*i,j*]quinoline (15). (1) To a solution of **14** (2.0 g, 11 mmol) in MeOH (110 mL) was added sodium cyanoborohydride (1.3 g, 34 mmol) within 20 min. After being stirred for 20 min, the mixture was acidified to pH 5 by acidic acid at 0 °C. After evaporation CH_2Cl_2 and H_2O were added to the residue. The organic layer was dried ($MgSO_4$) and evaporated and the residue was purified by flash chromatography (hexane/EtOAc 2/1) to give pure 4-(2-nitroethyl)pyrazolo[1,5-*a*]pyridine (1.7 g, 82%).

(2) To DMF (1 mL) was slowly added $POCl_3$ (88 μL, 0.96 mmol) under N_2 atmosphere. Then a solution of 4-(2-nitroethyl)pyrazolo[1,5-*a*]pyridine (160 mg, 0.83 mmol) in DMF (1 mL) was slowly added at 0 °C. The mixture was allowed to warm to room temperature and stirred for further 15 min. Then H_2O (0.17 mL, 9.2 mmol) and DMF (0.70 mL) were added. After 15 min a mixture of triethylamine (1.2 mL, 8.4 mmol) and MeOH (3.3 mL) was added at 0 °C. After 15 min saturated citric acid and ethyl acetate were added. The organic layer was dried ($MgSO_4$) and evaporated and the residue was purified by flash chromatography (EtOAc/hexane 2/8) to give pure **15** (86 mg, 51%) as a colorless solid (mp 202 °C). IR: 3354, 1634, 1588, 1463, 955 cm^{-1}. ^1H NMR ($CDCl_3$, 360 MHz) δ 4.53 (br s, 2H), 6.88 (dd, J = 7.1, 6.7 Hz, 1H), 7.05 (br d, J = 7.1 Hz, 1H), 7.94 (s, 1H), 8.12 (br s, 1H), 8.22 (br d, J = 6.7 Hz, 1H). MS m/z 201. Anal. ($C_{10}H_7N_3O_2$) C, H, N.

4-Amino-4,5-dihydro-3*H*-pyrazolo[4,5,1-*i,j*]quinoline (16). (1) To a solution of **15** (440 mg, 2.2 mmol) in MeOH (35 mL) was added sodium borohydride (1.3 g, 33 mmol) over 20 min. After further 20 min the mixture was acidified to pH 5 by acetic acid at 0 °C. Then the mixture was evaporated, and H_2O and CH_2Cl_2 were added to the residue. The organic layer was dried ($MgSO_4$) and evaporated and the residue was purified by flash chromatography (hexane/EtOAc 2/1) to give pure 4-nitro-4,5-dihydro-3*H*-pyrazolo[4,5,1-*i,j*]quinoline (360 mg, 81%) as a colorless solid.

(2) To a solution of 4-nitro-4,5-dihydro-3*H*-pyrazolo[4,5,1-*i,j*]quinoline (250 mg, 1.2 mmol) in EtOH (12 mL) were added tin powder (300 mg) and acetic acid (3 mL). The mixture was stirred at room temperature for 3 days. Then it was filtered with Celite and evaporated. After addition of water, aqueous NaOH (20%), and CH_2Cl_2, the organic layer was extracted with saturated NaCl solution. The organic layer was dried ($MgSO_4$) and evaporated and the residue was purified by flash chromatography (CH_2Cl_2/MeOH 8/2) to give pure **16**[21] (140 mg, 65%) as a colorless oil.

***N*-[(*N*′-Indan-2-yl-*N*′-propyl)-4-aminobutyl]methylcarboxamide (18).** A solution of (*N*-indan-2-yl-*N*-propyl)butane-1,4-diamine (103 mg, 0.42 mmol) (synthesized as previously described[56]) in $CHCl_3$ (10 mL) was cooled to 0 °C before triethylamine (100 μL, 0.72 mmol) and acetyl chloride (50 μL, 0.70 mmol) were added. Then the mixture was allowed to warm to room temperature and stirred for 3 h before another equivalent of acetyl chloride (50 μL, 0.70 mmol) was added. The mixture was stirred for a further 2 h. Then aqueous $NaHCO_3$ was added. The aqueous layer was extracted with CH_2Cl_2, and the combined organic layers were dried (Mg_2SO_4) and evaporated. The residue was purified by flash chromatography (CH_2Cl_2/MeOH 9/1 + 1% NEt_2Me) to give **18** as a brown oil (113 mg, 93%). IR 3297, 2956, 2935, 2870, 1651, 1558, 1460, 1369, 1297, 744, 638 cm^{-1}. ^1H NMR (360 MHz, $CDCl_3$) δ 0.89 (t, J = 7.4 Hz, 3H), 1.43−1.60 (m, 6H), 1.96 (s, 3H), 2.47−2.59 (m, 4H), 2.90 (dd, J = 15.4, 8.6 Hz, 2H), 3.03 (dd, J = 15.3, 7.7 Hz, 2H), 3.26 (m, 2H), 3.68 (m, 1H), 5.99 (m, 1H), 7.11−7.20 (m, 4H). ^{13}C NMR (90 MHz, $CDCl_3$) δ 12.0, 19.9, 23.4, 25.0, 27.8, 36.4, 39.6, 51.0, 53.3, 62.9, 124.5, 126.4, 141.7, 169.9. HR-EIMS calcd m/z for $C_{18}H_{28}N_2O$, 288.2202; found 288.2202.

***N*-[(*N*′-Indan-2-yl-*N*′-propyl)-4-aminobutyl]butylcarboxamide (19).** Compound **19** was prepared according to the protocol of **18** using a solution of (*N*-indan-2-yl-*N*-propyl)butane-1,4-diamine (146 mg, 0.59 mmol) (synthesized as previously described[56]) and triethylamine (150 μL, 1.1 mmol) and butyrylchloride (100 μL, 0.96 mmol). Purification by flash chromatography (hexane/EtOAc 1/2 + 0.5% NEt_2Me) gave **19** as a brown oil (46 mg, 24%). IR 3293, 3072, 2958, 2933, 2871, 1644, 1552, 1459, 1074, 742 cm^{-1}. ^1H NMR (360 MHz, $CDCl_3$) δ 0.88 (t, J = 7.3 Hz, 3H), 0.93 (t, J = 7.4 Hz, 3H), 1.43−1.55 (m, 4H), 1.60−1.71 (m, 4H), 2.12 (t, J = 7.5 Hz, 2H), 2.46−2.56 (m, 4H), 2.87 (dd, J = 15.4, 8.7 Hz, 2H), 3.01 (dd, J = 15.2, 7.7 Hz, 2H), 3.27 (m, 2H), 3.66 (m, 1H), 5.79 (m, 1H), 7.09−7.20 (m, 4H). ^{13}C NMR (90 MHz, $CDCl_3$) δ 12.0, 13.8, 19.2, 20.1, 25.0, 27.9, 36.5, 38.8, 39.4, 51.0, 53.4, 63.0, 124.4, 126.3, 141.8, 172.8. HR-EIMS calcd m/z for $C_{20}H_{32}N_2O$, 316.2515; found 316.2515.

***N*-[(*N*′-Indan-2-yl-*N*′-propyl)-4-aminobutyl]phenylcarboxamide (20).** Compound **20** was prepared according to the protocol of **18** using a solution of (*N*-indan-2-yl-*N*-propyl)butane-1,4-diamine (100 mg, 0.41 mmol) (synthesized as previously described[56]) and triethylamine (170 μL, 1.2 mmol) and benzoylchloride (50 μL, 0.41 mmol). Purification by flash chromatography (hexane/EtOAc 1/4 + 0.5% TEA) gave **20** as a colorless oil (45 mg, 24%). IR 3320, 2934, 2869, 1638, 1577, 1543, 1489, 1308, 1075 cm^{-1}. ^1H NMR (360 MHz, $CDCl_3$) δ 0.87 (t, J = 7.4 Hz, 3H), 1.49 (m, 2H), 1.72−1.55 (m, 4H), 2.52 (m, 2H), 2.58 (m, 2H), 2.87 (dd, J = 15.4, 8.6 Hz, 2H), 3.00 (dd, J = 15.2, 7.7 Hz, 2H), 3.48 (m, 2H), 3.68 (m, 1H), 6.51 (m, 1H), 7.09−7.19 (m, 4H), 7.35−7.50 (m, 3H), 7.71−7.86 (m, 2H). ^{13}C NMR (150 MHz, $CDCl_3$) δ 12.0, 19.9, 25.1, 27.8, 36.4, 40.1, 51.0, 53.4, 63.0, 124.4, 126.3, 126.9, 128.5, 131.2, 125.0, 141.8, 167.7. HR-EIMS calcd m/z for $C_{23}H_{30}N_2O$, 350.2358; found 350.2358.

Residue Numbering Scheme. For reasons of clarity amino acids positions are numbered according to Ballesteros and Weinstein.[60] Residues are numbered consecutively as [TM*x*].*n* relative to the most conserved residues within each TM, which is designed as [TM*x*].50.

Cell Culture and Transfection. Human embryonic kidney (HEK) 293 cells (American Type Culture Collection) were grown in DMEM/F-12 supplemented with 10% FBS, 2 mM L-glutamine, 1% penicillin−streptomycin. The cells were transiently transfected with the

corresponding cDNA by the $CaHPO_4$ method or using the TransIT-293 transfection reagent (Mirus Bio Corporation, Madison, WI). N-Terminal FLAG-tagged dopamine D_{2long} receptor constructs[61] were stably expressed in HEK 293 cells. For generation of stable monoclonal cell lines single colonies were chosen, propagated in the presence of selection-containing media (200 μg/mL Zeocin), and characterized for the expression of FLAG-D_{2long} receptor. The generation and maintenance of CHO cell stably expressing D_{2long}, D_{2short}, D_3, and $D_{4.4}$ receptor was described previously.[56,62−64]

Site Directed Mutagenesis. The D_3 receptor wild type and D_3D3.32E, D_3V2.61F, D_3L2.64F, D_3FV3.28,3.29LM, and D_3H6.55A mutants were generated as described previously.[16,38] The D_3S5.42A, D_3S5.46A, D_3F6.52W, D_3Y7.43A, and D_3Y7.43F were constructed using polymerase chain reaction (PCR) with the oligonucleotides (Supporting Information) bearing the desired mutation. The inserts bearing the desired mutations were cloned in the wild type vector using HindIII/BspEI (for the TM5 mutants), EcoRI/BspEI (for the TM6 and TM7 mutants). The entire coding region of the D_3 receptor clones was sequenced to ensure that the correct mutation was introduced and to confirm the absence of unwanted mutations.

Radioligand Displacement Studies on the Wild Type Receptors. Receptor binding studies were carried out as described.[65] In brief, competition binding experiments with the human D_{2long}, D_{2short}, D_3, and $D_{4.4}$ receptors were run on the membrane preparations from CHO cells stably expressing the corresponding receptor and [^{3}H]spiperone (specific activity of 84 Ci/mmol, PerkinElmer, Rodgau, Germany) at final concentrations of 0.1−0.5 nM according to the individual K_D values. Membranes, radioligand, and test compound were incubated for 60 min at 37 °C in binding buffer (50 mM Tris-HCl, 1 mM EDTA, 5 mM $MgCl_2$, 0.1 mM DL-dithiothreitol, 100 μg/mL bacitracin, 5 μg/mL soybean trypsin inhibitor; pH 7.4). The K_D values were 0.036−0.19, 0.070−0.24, 0.060−0.36, and 0.11−0.50 nM for the D_{2long}, D_{2short}, D_3, and D_4 receptor, respectively. The corresponding B_{max} values were in the range of 600−1600 fmol/mg for D_{2long}, 1100−2500 fmol/mg for D_{2short}, 1200−4200 fmol/mg for D_3, and 800−1600 fmol/mg for D_4 receptor, respectively. The assays were carried out in 96-well plates at protein concentrations of 2−20 μg/mL. Competition binding experiments at the high affinity binding site of the D_{2long} and the D_3 receptor were done using preparations from CHO cells stably expressing the corresponding receptor (protein concentrations of 200 and 2 μg/well for D_{2long} and D_3, respectively) and [^{3}H]7-OH-DPAT (specific activity of 50 Ci/mmol for D_3 and 161 Ci/mmol for D_{2long}; custom synthesis of [^{3}H](*R*)-(+)-7-OH-DPAT by Biotrend, Cologne, Germany) at final concentrations of 1.0 and 0.5 nM for D_{2long} and D_3, respectively. D_{2long} competition was done in 24-well plates at a final volume of 500 μL considering K_D of 1.2−1.4 nM and B_{max} of 145−260 fmol/mg while for D_3 binding a K_D of 0.66 nM and a B_{max} of 6000 fmol/mg was used. The D_1 and α1 receptor binding experiments were performed with homogenates prepared from porcine cerebral cortex as described.[66] Assays were run with membranes at protein concentrations per well of 40−60 μg/mL and radioligand concentrations of 0.2 nM [^{3}H]prazosin and 0.5 nM [^{3}H]SCH 23390 with K_D of 0.050−0.16 nM for the α1 receptor and 0.56−0.95 nM for the D_1 receptor. Protein concentration was established by the method of Lowry[67] using bovine serum albumin as a standard.

Membrane Preparations of Transiently Transfected HEK293 Cells. HEK 293 cells transiently transfected with the corresponding cDNA as indicated by $CaHPO_4$ method or using TransIT-293 transfection reagent (Mirus Corporation) were harvested 48 h after transfection. The medium was aspirated. Cells were washed once with the ice cold phosphate buffered saline (PBS, pH 7.4) and detached with the harvest buffer (10 mM Tris-HCl, 0.5 mM EDTA, 5.4 mM KCl, 140 mM NaCl, pH 7.4). The cells were scraped, collected in a centrifuge tube, and spun at 220*g* for 8 min. The resulting pellet was resuspended in 5 mL of the homogenate buffer (50 mM Tris-HCl, 5 mM EDTA, 1.5 mM $CaCl_2$, 5 mM $MgCl_2$, 5 mM KCl, 120 mM NaCl, pH 7.4) and subsequently lysed with an Ultraturrax. After additional centrifugation at 50000*g*, the membranes were resuspended in binding buffer (50 mM Tris, 1 mM EDTA, 5 mM $MgCl_2$, 100 μg/mL bacitracin, 5 μg/mL soybean trypsin inhibitor) and homogenized 10 times with a glass−Teflon homogenizer at 4 °C. The homogenized membranes were shock-frozen in liquid nitrogen and stored at −80 °C. The protein concentration was determined with the Lowry method[67] using bovine serum albumin as a standard.

Radioligand Displacement Studies on the Membrane Preparations of Transiently Transfected Cells. The radioligand [^{3}H]spiperone was used to determine the K_d and B_{max} values for the membrane preparations of transiently transfected HEK 293 cells expressing the D_3 wild type and mutant receptors from saturation experiments, and the K_i values for the compounds were obtained by competition experiments.[65] Briefly, the assays were carried out in the 96-well plates at a protein concentration of 20−200 μg/mL in a final volume of 200 μL. After incubation for 1 h at 37 °C the assay was stopped by filtration through Whatman GF/B filters presoaked with 0.3% polyethylenimine. The filters were rinsed 5 times with ice cold Tris-NaCl buffer. After 3 h of drying at 60 °C filters were sealed with melt-on scintillator sheets MeltiLex B/HS (PerkinElmer, Rodgau, Germany) and the filter-bound radioactivity was measured in a MicroBeta TriLux liquid scintillator counter (PerkinElmer, Rodgau, Germany). Three to six experiments per compound were performed with each concentration in triplicate.

[^{35}S]GTPγS Incorporation Assay. The [^{35}S]GTPγS binding assay was performed on membrane preparations of transiently transfected HEK293 cells that expressed the corresponding dopamine receptor and the pertussin toxin insensitive Gα protein (D_{2long} + $G\alpha_o$, D_{2long} + $G\alpha_{i2}$, or D_3 + $G\alpha_o$). The receptor expression was determined in saturation experiments (1500 ± 50, 4900 ± 440, and 1100 ± 90 fmol/mg protein, respectively). The assay was carried out in 96-well plates at the final volume of 200 μL. The incubation buffer contained 20 mM Hepes, 10 mM $MgCl_2 \cdot 6H_20$,100 mM NaCl, and 70 mg/L saponin (pH 7.4).[68] Membranes (30−50 μg/mL of membrane protein), compounds, and 10 μM GDP were preincubated in the absence of [^{35}S]GTPγS for 30 min at 37 or 30 °C (for $D_{2\ L}$ + $G\alpha_{i2}$). After the addition of 0.10 nM [^{35}S]GTPγS membranes were incubated for an additional 30 min at 37 °C or 75 min at 30 °C (for $D_{2\ L}$ + $G\alpha_{i2}$). Longer incubation period for the $D_{2\ L}$ + $G\alpha_{i2}$ pair is necessary because both the dissociation of GDP from $G\alpha_{i2}$ and the association of [^{35}S]GTPγS to $G\alpha_{i2}$ are 2−3 times slower than for $G\alpha_o$.[69] Incubation was terminated by filtration through Whatman GF/B filters soaked with ice cold PBS. The filter-bound radioactivity was measured as described above. Three to four experiments per compound were performed with each concentration in eight replicates.

Adenylyl Cyclase Inhibition Assay. Bioluminescence based cAMP-Glo assay (Promega, Mannheim, Germany) was performed according to the manufacturer's instructions. Briefly, CHO cells expressing D_{2long} and D_3 wild type receptor were seeded into a white half-area 96-well plate (5000 cells/well) 24 h prior to the assay. On the day of the assay cells were first briefly washed with phosphate buffered saline (PBS, pH 7.4) to remove traces of serum and incubated with various concentrations of compounds in the presence of 20 μM (for D_{2long}) or 2 μM (for D_3) forskolin in serum-free medium that contained 500 μM IBMX and 100 μM Ro 20-1724 at pH 7.4. After 15 min of incubation at 25 °C the cells were lysed with cAMP-Glo lysis buffer. After lysis the kinase reaction was performed with a reaction buffer containing PKA. At the end of the kinase reaction an equal volume of Kinase-Glo reagent was added. The plates were read with a luminescence protocol on a microplate reader Victor^{3}V (Perkin-Elmer, Rodgau, Germany). The experiments were performed three to nine times per compound with each concentration in triplicate.

[^{3}H]Thymidine Incorporation Assay. Determination of ligand efficacy of representative compounds was carried out by measuring the incorporation of [^{3}H]thymidine into proliferating cells after stimulation with the test compound as described in the literature.[70,71] For this assay D_3 expressing CHO dhfr$^-$ cells or D_{2long} expressing CHO10001 cells have been incubated with 0.02 μCi [^{3}H]thymidine per well (specific activity 25 μCi/mmol, Biotrend, Cologne, Germany) for 2 h. Dose-response curves of 6−11 experiments have been normalized and pooled to get a mean curve from which the EC_{50} value and the maximum intrinsic activity of each compound could be compared to the effects of the full agonist quinpirole.

Data Analysis. The resulting competition curves of the receptor binding experiments and activity assays were analyzed by nonlinear regression using the algorithms in PRISM 5.0 (GraphPad Software, San Diego, CA). Competition curves were fitted to the sigmoid curve by nonlinear regression analysis in which the log EC_{50} and the Hill coefficient were free parameters. EC_{50} values were transformed to K_i values according to the equation of Cheng and Prusoff.[72] For the receptor binding experiments (number of experiments ≥3, regardless of number of replicates), standard error of mean was calculated. In the case were only two experiments were performed (because of poor binding affinity of a compound), standard deviation was calculated. The data obtained from functional assay were normalized (using reference agonist quinpirole to set 0% and 100%) and pooled, and the 95% confidential interval for EC_{50} values and efficacy were estimated. Dose-response curves of activity assays were fitted to the operational model developed by Black and Leff[28] to obtain an estimate of the transducer constant τ:

$$E = \frac{E_m \tau^n [A^n]}{(K_A + [A])^n + \tau^n [A]^n} \quad (1)$$

with E denoting the effect, E_m the maximum possible effect, [A] the agonist concentration, and K_A the dissociation constant of the agonist−receptor complex. The transducer constant τ is a parameter describing the signal transduction efficiency of the system, and the intrinsic efficacy of the agonist is estimated from the fit of the data. Quinpirole was used as the reference full agonist, defining zero and a maximal (100%) response of the system. The curves of all agonists had a Hill coefficient of unity or close to unity. The $\log(\tau/K_A)$ values were calculated, which depicted the "strength" of a given agonist to activate a defined pathway in a defined system.[31,73] The $\Delta \log(\tau/K_A)$ values were calculated as

$$\Delta \log(\tau/K_A)_{\text{agonist/reference}} = \log(\tau/K_A)_{\text{agonist}} - \log(\tau/K_A)_{\text{reference}} \quad (2)$$

to compare various agonists within signaling pathway. The difference of the $\Delta \log(\tau/K_A)$ between selected pathways yields $\Delta\Delta \log(\tau/K_A)$, which describes agonist bias or functional selectivity of a given ligand.

Immunocytochemistry. The antibody-feeding immunocytochemistry experiments were performed as previously described.[74] Briefly, cells stably expressing the FLAG-tagged D_{2long} receptor (or the HA-tagged D_3 receptor) were grown on coverslips pretreated with gelatin to ∼50% confluency. Live cells were fed M1 antibody (Sigma) directed against the FLAG epitope or HA-11 antibody directed against the FLAG epitope (Covance) (1:1000, 30 min) and then incubated with ligands (10 μM, 30 min) or left untreated. Quinpirole (10 μM, 30 min), **2** (10 μM), and **5a** (10 μM) were used. Cells were then fixed with 4% formaldehyde in PBS, pH 7.4. After fixation cells were permeabilized in BLOTTO (3% milk, 0.1% Triton X, 1 mM $CaCl_2$, 50 mM Tris-HCl, pH 7.5) and stained with Alexa Fluor 594 goat anti-mouse IgG2b or AlexaFluor 594 goat anti-mouse IgG1 antibody (Invitrogen, 1:500, 45 min). The coverslips were mounted using mounting media from Vectashield. Mounted sections were examined by using LSM 510 laser confocal microscope (Zeiss).

Biotin Protection/Degradation Assay. HEK 293 cells stably expressing the N-terminally FLAG tagged D_{2long} receptor were grown to 80% confluency in poly-D-lysine pretreated 10 cm plates and subjected to the biotin protection/degradation assay protocol as described.[74] Cells were left untreated or stimulated for 30 min with 10 μM quinpirole, 10 μM **2**, or 10 μM **5a**. Briefly, cells were treated with 3 μg/mL disulfide-cleavable biotin (Pierce) for 30 min at 4 °C. Cells were then washed in PBS and placed in prewarmed medium for 15 min before treatment with ligand (or no treatment) for 30 min. Concurrent with ligand treatment, 100% and strip plates remained at 4 °C. After ligand treatment, plates were washed with PBS and remaining cell surface-biotinylated receptors were stripped in 50 mM glutathione, 0.3 M NaCl, 75 mM NaOH, 1% fetal bovine serum at 4 °C for 30 min. Cells were quenched with PBS containing 50 mM iodoacetamide and 1% bovine serum albumin and then lysed in 0.1% Triton X-100, 150 mM NaCl, 25 mM KCl, 10 mM Tris-HCl, pH 7.4, with protease inhibitors (Roche Applied Science, Basel, Switzerland). Cleared lysates were incubated with M2 anti-FLAG affinity resin (Sigma) overnight at 4 °C, washed extensively, and deglycosylated with PNGase F (New England Biolabs) for 2 h at 37 °C. Samples were denatured in SDS sample buffer with no reducing agent added, resolved by SDS-PAGE using 8−16% Tris-glycine precast gels (Invitrogen), transferred to the PVDF membrane, overlaid with streptavidin (Vectastain ABC immunoperoxidase reagent, Vector Laboratories, Burlingame, CA), and finally developed with enhanced chemiluminescence reagent (Invitrogen). For quantification, data generated on three independent blots were analyzed using ImageJ software, where the nontreatment was designated as 0% and treatment with quinpirole for 30 min was designated as 100% signal.

Docking Procedure. The recently published crystal structure of the dopamine D_3 receptor[20] was used for docking investigations. Compounds **2**, (***R***)-**5a**, and (***S***)-**5a** were geometry optimized by means of Gaussian 98 at the 6-31** level.[75] A formal charge of +1 was attributed to the ligands because the tertiary amine of (***R***)-**5a** and (***S***)-**5a** and the piperazine nitrogen connected to the aliphatic chain of **2** are assumed to be protonated at physiological pH. The protonation of (***R***)-**5a** and (***S***)-**5a** resulted in two stereoisomers.

The ligands were then docked into the crystal structure of the dopamine D_3 receptor[20] using the program AUTODOCK4.[49−51] To completely enclose the binding site crevice, which is defined by the extracellular parts of TM2, TM3, TM5, TM6, and TM7, a grid of 70 points in each of the *x*, *y*, and *z* directions and a grid spacing of 0.375 Å were applied. The AUTODOCK Lamarckian genetic algorithm with a randomly selected starting position was used to generate 50 docking conformations of each compound that were clustered manually and scored by DrugScore^{online}, applying the knowledge-based DrugScore^{CSD} scoring function.[53] On the basis of this scoring, the best conformation of each cluster was selected. A final selection was made according to experimental data (site-directed mutagenesis and radioligand displacement studies).

Analysis of the docking poses of the two stereoisomers of (***R***)-**5a** and (***S***)-**5a**, which were generated by the protonation of the tertiary amine, showed that only the *R*-enantiomer possesses the possibility to position the propyl moiety in the "propyl cleft", which has been proposed to extend from TM3 toward TM2 and TM7.[52] Therefore, the *R*-enantiomer of (***R***)-**5a** and (***S***)-**5a** was chosen for further analysis. In addition, docking of compounds (***R***)-**5a** and (***S***)-**5a** resulted in two ligand−receptor complexes in each case, which showed distinct position and orientation of the tetrahydropyrazolopyridine moiety. All four complexes were considered for further analysis.

After the selection of the final docking pose, the receptor−ligand complexes of **2**, (***R***)-**5a**, and (***S***)-**5a** were subjected to energy minimization using the SANDER classic module of AMBER 10.[76] For the energy minimization of (***R***)-**5a** and (***S***)-**5a**, the side chain conformation of Ser5.43 was rearranged in accordance with the crystal structure of the

β_2-adrenergic receptor bound to the agonist FAUC 50.[54] The side chain conformation of Ser5.43 enabled a hydrogen bond interaction with the tetrahydropyrazolopyridine moiety in addition to the interaction between Ser5.42 and this moiety. Then 500 cycles of steepest descent minimization were applied, followed by 4500 cycles of conjugate gradient minimization. All calculations were carried out in a water box with periodic boundary conditions and a nonbonded cutoff of 8.0 Å. The all atom force field ff99SB was applied.[77] Parametrization of the compounds was accomplished with antechamber. The charges for the ligand atoms were calculated using Gaussian 98, with a 6-31** basis set, and then the RESP procedure was applied as described in the literature.[75,78]

■ ASSOCIATED CONTENT

Supporting Information. Experimental data, results of functional assays and site directed mutagenesis, binding data, and results from operational model. This material is available free of charge via the Internet at http://pubs.acs.org.

■ AUTHOR INFORMATION

Corresponding Author
*Phone: +49(9131)852-9383. Fax. +49(9131)852-2585. E-mail: peter.gmeiner@medchem.uni-erlangen.de.

■ ACKNOWLEDGMENT

We thank Prof. Graeme Milligan (University of Glasgow, U.K.) for providing us with the cDNA for $G\alpha_{o1}$ or $G\alpha_{i2}$ proteins, and we thank Raquel Ortega for the synthesis of a molecular probe.

■ ABBREVIATIONS USED

7TM, seven transmembrane; TM, transmembrane; SCH 23390, 7-chloro-3-methyl-1-phenyl-1,2,4,5-tetrahydro-3-benzazepin-8-ol; spiperone, 8-[4-(4-fluorophenyl)-4-oxo-butyl]-1-phenyl-1,3, 8-triazaspiro[4.5]decan-4-one; WAY100635, *N*-[2-[4-(2-methoxyphenyl)-1-piperazinyl]ethyl]-*N*-(2-pyridyl)cyclohexanecarboxamide; prazosin, 2-[4-(2-furoyl)piperazin-1-yl]-6,7-dimethoxyquinazolin-4-amine; EDTA, ethylenediaminetetraacetic acid; 7-OH-DPAT, 7-hydroxy-2-(*N*,*N*-di-*n*-propylamino)tetralin; IBMX, 3-isobutyl-1-methylxanthine; Ro 20-1724, [4-(3-butoxy-4-methoxybenzyl)imidazoline; CHO, Chinese hamster ovary; HEK, human embryonic kidney; FBS, fetal bovine serum; PBS, phosphate buffered saline; ELISA, enzyme-linked immunosorbent assay; SDS-PAGE, sodium dodecyl sulfate polyacrylamide gel electrophoresis; PVDF, polyvinylidene fluoride; EC_{50}, half maximal effective concentration; PKA, protein kinase A; MAPK, mitogene-activated protein kinase; ERK1/2, extracellular regulated kinase 1/2; SAR, structure−activity relationships; NMR, nuclear magnetic resonance; MHz, megahertz; LC/MS, liquid chromatography/mass spectrometry; APC, atmospheric pressure chemical; TLC, thin layer chromatography; HRMS, high resolution mass spectrometry; HPLC, high performance liquid chromatography; EIMS, electron ionization mass spectrometry; DMF, dimethylformamide

■ REFERENCES

(1) Neve, K. A.; Seamans, J. K.; Trantham-Davidson, H. Dopamine Receptor Signaling. *J. Recept. Signal Transduction Res.* **2004**, *24*, 165–205.
(2) Hindle, J. V. Ageing, Neurodegeneration and Parkinson's Disease. *Age Ageing* **2010**, *39*, 156–161.
(3) Schetz, J. A. Pharmacotherapies for the Management of Parkinson's Disease. *Drug Topics* **2001**, *19*, 52–61.
(4) Mayeux, R.; Denaro, J.; Hemenegildo, N.; Marder, K.; Tang, M.-X.; Cote, L. J.; Stern, Y. A Population-Based Investigation of Parkinson's Disease with and without Dementia: Relationship to Age and Gender. *Arch. Neurol.* **1992**, *49*, 492–497.
(5) Lieberman, A.; Ranhosky, A.; Korts, D. Clinical Evaluation of Pramipexole in Advanced Parkinson's Disease: Results of a Double-Blind, Placebo-Controlled, Parallel-Group Study. *Neurology* **1997**, *49*, 162–168.
(6) Boeckler, F.; Leng, A.; Mura, A.; Bettinetti, L.; Feldon, J.; Gmeiner, P.; Ferger, B. Attenuation of 1-Methyl-4-phenyl-1,2,3,6-tetrahydropyridine (MPTP) Neurotoxicity by the Novel Selective Dopamine D3-Receptor Partial Agonist FAUC 329 Predominantly in the Nucleus Accumbens of Mice. *Biochem. Pharmacol.* **2003**, *66*, 1025–1032.
(7) Le, W. D.; Jankovic, J. Are Dopamine Receptor Agonists Neuroprotective in Parkinson's Disease? *Drugs Aging* **2001**, *18*, 389–396.
(8) van Vliet, L. A.; Rodenhuis, N.; Dijkstra, D.; Wikstrom, H.; Pugsley, T. A.; Serpa, K. A.; Meltzer, L. T.; Heffner, T. G.; Wise, L. D.; Lajiness, M. E.; Huff, R. M.; Svensson, K.; Sundell, S.; Lundmark, M. Synthesis and Pharmacological Evaluation of Thiopyran Analogues of the Dopamine D3 Receptor-Selective Agonist (4a*R*,10b*R*)-(+)-*trans*-3,4,4a,10b-Tetrahydro-4-*n*-propyl-2*H*,5*H*-[1]benzopyrano[4,3-*b*]-1,4-oxazin-9-ol (PD 128907). *J. Med. Chem.* **2000**, *43*, 2871–2882.
(9) Wikstroem, H.; Andersson, B.; Sanchez, D.; Lindberg, P.; Arvidsson, L. E.; Johansson, A. M.; Nilsson, J. L. G.; Svensson, K.; Hjorth, S.; Carlsson, A. Resolved Monophenolic 2-Aminotetralins and 1,2,3,4,4a,5,6,10b-Octahydrobenzo[*f*]quinolines: Structural and Stereochemical Considerations for Centrally Acting Pre- and Postsynaptic Dopamine-Receptor Agonists. *J. Med. Chem.* **1985**, *28*, 215–225.
(10) Titus, R. D.; Kornfeld, E. C.; Jones, N. D.; Clemens, J. A.; Smalstig, E. B.; Fuller, R. W.; Hahn, R. A.; Hynes, M. D.; Mason, N. R. Resolution and Absolute Configuration of an Ergoline-Related Dopamine Agonist, *trans*-4,4a,5,6,7,8,8a,9-Octahydro-5-propyl-1*H*(or 2*H*)-pyrazolo[3,4-*g*]quinoline. *J. Med. Chem.* **1983**, *26*, 1112–1116.
(11) Malmberg, A.; Hook, B. B.; Johansson, A. M.; Hacksell, U. Novel (*R*)-2-Amino-5-fluorotetralins: Dopaminergic Antagonists and Inverse Agonists. *J. Med. Chem.* **1996**, *39*, 4421–4429.
(12) Hackling, A.; Ghosh, R.; Perachon, S.; Mann, A.; Holtje, H. D.; Wermuth, C. G.; Schwartz, J. C.; Sippl, W.; Sokoloff, P.; Stark, H. *N*-(omega-(4-(2-Methoxyphenyl)piperazin-1-yl)alkyl)carboxamides as dopamine D2 and D3 receptor ligands. *J. Med. Chem.* **2003**, *46*, 3883–3899.
(13) Boeckler, F.; Gmeiner, P. Dopamine D3 Receptor Ligands—Recent Advances in the Control of Subtype Selectivity and Intrinsic Activity. *Biochim. Biophys. Acta, Biomembr.* **2007**, *1768*, 871–887.
(14) Löber, S.; Hübner, H.; Tschammer, N.; Gmeiner, P. Recent Advances in the Search for D3- and D4-Selective Drugs: Probes, Models and Candidates *Trends Pharmacol. Sci.* [Online early access]. Published Online: January 11, **2011**.
(15) Huber, D.; Hübner, H.; Gmeiner, P. 1,1′-Disubstituted Ferrocenes as Molecular Hinges in Mono- and Bivalent Dopamine Receptor Ligands. *J. Med. Chem.* **2009**, *52*, 6860–6870.
(16) Dörfler, M.; Tschammer, N.; Hamperl, K.; Hübner, H.; Gmeiner, P. Novel D3 Selective Dopaminergics Incorporating Enyne Units as Nonaromatic Catechol Bioisosteres: Synthesis, Bioactivity, and Mutagenesis Studies. *J. Med. Chem.* **2008**, *51*, 6829–6838.
(17) Avenell, K. Y.; Boyfield, I.; Hadley, M. S.; Johnson, C. N.; Nash, D. J.; Riley, G. J.; Stemp, G. Heterocyclic Analogues of 2-Aminotetralins with High Affinity and Selectivity for the Dopamine D3 Receptor. *Bioorg. Med. Chem. Lett.* **1999**, *9*, 2715–2720.
(18) Boyfield, I.; Coldwell, M. C.; Hadley, M. S.; Johnson, C. N.; Riley, G. J.; Scott, E. E.; Stacey, R.; Stemp, G.; Thewlis, K. M. A Novel Series of 2-Aminotetralins with High Affinity and Selectivity for the Dopamine D3 Receptor. *Bioorg. Med. Chem. Lett.* **1997**, *7*, 1995–1998.
(19) Elsner, J.; Boeckler, F.; Heinemann, F. W.; Hübner, H.; Gmeiner, P. Pharmacophore-Guided Drug Discovery Investigations Leading to Bioactive 5-Aminotetrahydropyrazolopyridines. Implications

for the Binding Mode of Heterocyclic Dopamine D3 Receptor Agonists. *J. Med. Chem.* **2005**, *48*, 5771–5779.

(20) Chien, E. Y. T.; Liu, W.; Zhao, Q.; Katritch, V.; Won Han, G.; Hanson, M. A.; Shi, L.; Newman, A. H.; Javitch, J. A.; Cherezov, V.; Stevens, R. C. Structure of the Human Dopamine D3 Receptor in Complex with a D2/D3 Selective Antagonist. *Science* **2010**, *330*, 1091–1095.

(21) Gmeiner, P.; Sommer, J.; Mierau, J.; Höfner, G. Dopamine Autoreceptor Agonists: Computational Studies, Synthesis and Biological Investigations. *Bioorg. Med. Chem. Lett.* **1993**, *3*, 1477–1483.

(22) Bach, N. J.; Kornfeld, E. C.; Jones, N. D.; Chaney, M. O.; Dorman, D. E.; Paschal, J. W.; Clemens, J. A.; Smalstig, E. B. Bicyclic and Tricyclic Ergoline Partial Structures. Rigid 3-(2-Aminoethyl)pyrroles and 3- and 4-(2-Aminoethyl)pyrazoles as Dopamine Agonists. *J. Med. Chem.* **1980**, *23*, 481–491.

(23) Stemp, G.; Johnson, C. N. Preparation of Bicyclic Amine Derivatives and Their Use as Dopamine D3-Receptor (Ant)Agonist Antipsychotic Agents. WO9630333, 1996.

(24) Löber, S.; Ortner, B.; Bettinetti, L.; Hübner, H.; Gmeiner, P. Analogs of the Dopamine D4 Receptor Ligand FAUC 113 with Planar- and Central-Chirality. *Tetrahedron: Asymmetry* **2002**, *13*, 2303–2310.

(25) van Vliet, L. A.; Tepper, P. G.; Dijkstra, D.; Damsma, G.; Wikstrom, H.; Pugsley, T. A.; Akunne, H. C.; Heffner, T. G.; Glase, S. A.; Wise, L. D. Affinity for Dopamine D2, D3, and D4 Receptors of 2-Aminotetralins. Relevance of D2 Agonist Binding for Determination of Receptor Subtype Selectivity. *J. Med. Chem.* **1996**, *39*, 4233–4237.

(26) Lane, J. R.; Powney, B.; Wise, A.; Rees, S.; Milligan, G. G Protein Coupling and Ligand Selectivity of the D2L and D3 Dopamine Receptors. *J. Pharmacol. Exp. Ther.* **2008**, *325*, 319–330.

(27) Cordeaux, Y.; Nickolls, S. A.; Flood, L. A.; Graber, S. G.; Strange, P. G. Agonist Regulation of D2 Dopamine Receptor/G Protein Interaction: Evidence for Agonist Selection of G Protein Subtype. *J. Biol. Chem.* **2001**, *276*, 28667–28675.

(28) Black, J. W.; Leff, P. Operational Models of Pharmacological Agonism. *Proc. R. Soc., Ser. B* **1983**, *220*, 141–162.

(29) Tschammer, N.; Bollinger, S.; Kenakin, T.; Gmeiner, P. Histidine 6.55 Is a Major Determinant of Ligand Biased Signaling in Dopamine D2L Receptor. *Mol. Pharmacol.* **2011**, *79*, 575–585.

(30) Evans, B. A.; Broxton, N.; Merlin, J.; Sato, M.; Hutchinson, D. S.; Christopoulos, A.; Summers, R. J. Quantification of Functional Selectivity at the Human Alpha1A-Adrenoceptor. *Mol. Pharmacol.* **2011**, *79*, 298–307.

(31) Kenakin, T. P. '7TM Receptor Allostery: Putting Numbers to Shapeshifting Proteins. *Trends. Pharmacol. Sci.* **2009**, *30*, 460–469.

(32) Gay, E. A.; Urban, J. D.; Nichols, D. E.; Oxford, G. S.; Mailman, R. B. Functional Selectivity of D2 receptor Ligands in a Chinese Hamster Ovary hD2L Cell Line: Evidence for Induction of Ligand-Specific Receptor States. *Mol. Pharmacol.* **2004**, *66*, 97–105.

(33) Lane, J. R.; Powney, B.; Wise, A.; Rees, S.; Milligan, G. Protean Agonism at the Dopamine D2 Receptor: (*S*)-3-(3-Hydroxyphenyl)-*N*-propylpiperidine Is an Agonist for Activation of Go1 but an Antagonist/Inverse Agonist for Gi1,Gi2, and Gi3. *Mol. Pharmacol.* **2007**, *71*, 1349–1359.

(34) Chen, J.; Collins, G. T.; Zhang, J.; Yang, C.-Y.; Levant, B.; Woods, J.; Wang, S. Design, Synthesis, and Evaluation of Potent and Selective Ligands for the Dopamine 3 (D3) Receptor with a Novel in Vivo Behavioral Profile. *J. Med. Chem.* **2008**, *51*, 5905–5908.

(35) Bartlett, S. E.; Enquist, J.; Hopf, F. W.; Lee, J. H.; Gladher, F.; Kharazia, V.; Waldhoer, M.; Mailliard, W. S.; Armstrong, R.; Bonci, A.; Whistler, J. L. Dopamine Responsiveness Is Regulated by Targeted Sorting of D2 Receptors. *Proc. Natl. Acad. Sci. U.S.A.* **2005**, *102*, 11521–11526.

(36) Thompson, D.; Whistler, J. L. Dopamine D3 Receptors Are Down-Regulated following Heterologous Endocytosis by a Specific Interaction with G Protein-Coupled Receptor-Associated Sorting Protein-1. *J. Biol. Chem.* **2011**, *286*, 1598–1608.

(37) Cho, E.-Y.; Cho, D.-I.; Park, J. H.; Kurose, H.; Caron, M. G.; Kim, K.-M. Roles of Protein Kinase C and Actin-Binding Protein 280 in the Regulation of Intracellular Trafficking of Dopamine D3 Receptor. *Mol. Endocrinol.* **2007**, *21*, 2242–2254.

(38) Ehrlich, K.; Götz, A.; Bollinger, S.; Tschammer, N.; Bettinetti, L.; Härterich, S.; Hübner, H.; Lanig, H.; Gmeiner, P. Dopamine D2, D3, and D4 Selective Phenylpiperazines as Molecular Probes To Explore the Origins of Subtype Specific Receptor Binding. *J. Med. Chem.* **2009**, *52*, 4923–4935.

(39) Sartania, N.; Strange, P. G. Role of Conserved Serine Residues in the Interaction of Agonists with D3 Dopamine Receptors. *J. Neurochem.* **1999**, *72*, 2621–2624.

(40) Xhaard, H.; Rantanen, V. V.; Nyronen, T.; Johnson, M. S. Molecular Evolution of Adrenoceptors and Dopamine Receptors: Implications for the Binding of Catecholamines. *J. Med. Chem.* **2006**, *49*, 1706–1719.

(41) Wiens, B. L.; Nelson, C. S.; Neve, K. A. Contribution of Serine Residues to Constitutive and Agonist-Induced Signaling via the D2S Dopamine Receptor: Evidence for Multiple, Agonist-Specific Active Conformations. *Mol. Pharmacol.* **1998**, *54*, 435–444.

(42) Schwartz, T. W.; Frimurer, T. M.; Holst, B.; Rosenkilde, M. M.; Elling, C. E. Molecular Mechanism of 7TM Receptor Activation—A Global Toggle Switch Model. *Annu. Rev. Pharmacol. Toxicol.* **2006**, *46*, 481–519.

(43) Elling, C. E.; Frimurer, T. M.; Gerlach, L.-O.; Jorgensen, R.; Holst, B.; Schwartz, T. W. Metal Ion Site Engineering Indicates a Global Toggle Switch Model for Seven-Transmembrane Receptor Activation. *J. Biol. Chem.* **2006**, *281*, 17337–17346.

(44) Bokoch, M. P.; Zou, Y.; Rasmussen, S. G.; Liu, C. W.; Nygaard, R.; Rosenbaum, D. M.; Fung, J. J.; Choi, H. J.; Thian, F. S.; Kobilka, T. S.; Puglisi, J. D.; Weis, W. I.; Pardo, L.; Prosser, R. S.; Mueller, L.; Kobilka, B. K. Ligand-Specific Regulation of the Extracellular Surface of a G-Protein-Coupled Receptor. *Nature* **2010**, *463*, 108–112.

(45) Nygaard, R.; Frimurer, T. M.; Holst, B.; Rosenkilde, M. M.; Schwartz, T. W. Ligand Binding and Micro-Switches in 7TM Receptor Structures. *Trends Pharmacol. Sci.* **2009**, *30*, 249–259.

(46) Schetz, J. A.; Benjamin, P. S.; Sibley, D. R. Nonconserved Residues in the Second Transmembrane-Spanning Domain of the D4 Dopamine Receptor Are Molecular Determinants of D4-Selective Pharmacology. *Mol. Pharmacol.* **2000**, *57*, 144–152.

(47) Simpson, M. M.; Ballesteros, J. A.; Chiappa, V.; Chen, J.; Suehiro, M.; Hartman, D. S.; Godel, T.; Snyder, L. A.; Sakmar, T. P.; Javitch, J. A. Dopamine D4/D2 Receptor Selectivity Is Determined by a Divergent Aromatic Microdomain Contained within the Second, Third, and Seventh Membrane-Spanning Segments. *Mol. Pharmacol.* **1999**, *56*, 1116–1126.

(48) Kortagere, S.; Gmeiner, P.; Weinstein, H.; Schetz, J. A. Certain 1,4-Disubstituted Aromatic Piperidines and Piperazines with Extreme Selectivity for the Dopamine D4 Receptor Interact with a Common Receptor Microdomain. *Mol. Pharmacol.* **2004**, *66*, 1491–1499.

(49) Morris, G. M.; Goodsell, D. S.; Halliday, R. S.; Huey, R.; Hart, W. E.; Belew, R. K.; Olson, A. J. Automated Docking Using a Lamarckian Genetic Algorithm and an Empirical Binding Free Energy Function. *J. Comput. Chem.* **1998**, *19*, 1639–1662.

(50) Sanner, M. F. Phyton: A Programming Language for Software Integration and Development. *J. Mol. Graphics Modell.* **1999**, *17*, 57–61.

(51) Huey, R.; Morris, G. M.; Olson, A. J.; Goodsell, D. S. A Semiempirical Free Energy Force Field with Charge-Based Desolvation. *J. Comput. Chem.* **2007**, *28*, 1145–1152.

(52) Malmberg, A.; Nordvall, G.; Johansson, A. M.; Mohell, N.; Hacksell, U. Molecular Basis for the Binding of 2-Aminotetralins to Human Dopamine D2A and D3 Receptors. *Mol. Pharmacol.* **1994**, *46*, 299–312.

(53) Velec, H. F.; Gohlke, H.; Klebe, G. DrugScore(CSD)-Knowledge-Based Scoring Function Derived from Small Molecule Crystal Data with Superior Recognition Rate of Near-Native Ligand Poses and Better Affinity Prediction. *J. Med. Chem.* **2005**, *48*, 6296–303.

(54) Rosenbaum, D. M.; Zhang, C.; Lyons, J. A.; Holl, R.; Aragao, D.; Arlow, D. H.; Rasmussen, S. G. F.; Choi, H.-J.; DeVree, B. T.; Sunahara, R. K.; Chae, P. S.; Gellman, S. H.; Dror, R. O.; Shaw, D. E.; Weis, W. I.;

Caffrey, M.; Gmeiner, P.; Kobilka, B. K. Structure and Function of an Irreversible Agonist-[beta]2 Adrenoceptor Complex. *Nature* **2011**, *469*, 236–240.

(55) Cannon, J. G.; Perez, J. A.; Pease, J. P.; Long, J. P.; Flynn, J. R.; Rusterholz, D. B.; Dryer, S. E. Comparison of Biological Effects of N-Alkylated Congeners of Beta-Phenethylamine Derived from 2-Aminotetralin, 2-Aminoindan, and 6-Aminobenzocycloheptene. *J. Med. Chem.* **1980**, *23*, 745–749.

(56) Tschammer, N.; Dörfler, M.; Hübner, H.; Gmeiner, P. Engineering a GPCR−Ligand Pair That Simulates the Activation of D2L by Dopamine. *ACS Chem. Neurosci.* **2010**, *1*, 25–35.

(57) Rosenkilde, M. M.; Benned-Jensen, T.; Frimurer, T. M.; Schwartz, T. W. The Minor Binding Pocket: A Major Player in 7TM Receptor Activation. *Trends. Pharmacol. Sci.* **2010**, *31*, 567–574.

(58) Rasmussen, S. G. F.; Choi, H.-J.; Fung, J. J.; Pardon, E.; Casarosa, P.; Chae, P. S.; DeVree, B. T.; Rosenbaum, D. M.; Thian, F. S.; Kobilka, T. S.; Schnapp, A.; Konetzki, I.; Sunahara, R. K.; Gellman, S. H.; Pautsch, A.; Steyaert, J.; Weis, W. I.; Kobilka, B. K. Structure of a Nanobody-Stabilized Active State of the [beta]2 Adrenoceptor. *Nature* **2011**, *469*, 175–180.

(59) Warne, T.; Moukhametzianov, R.; Baker, J. G.; Nehme, R.; Edwards, P. C.; Leslie, A. G. W.; Schertler, G. F. X.; Tate, C. G. The Structural Basis for Agonist and Partial Agonist Action on a [beta]1-Adrenergic Receptor. *Nature* **2011**, *469*, 241–244.

(60) Ballesteros, J. A.; Weinstein, H. Integrated Methods for Modeling G-Protein Coupled Receptors. *Methods Neurosci.* **1995**, *25*, 366–428.

(61) Vickery, R. G.; von Zastrow, M. Distinct Dynamin-Dependent and -Independent Mechanisms Target Structurally Homologous Dopamine Receptors to Different Endocytic Membranes. *J. Cell Biol.* **1999**, *144*, 31–43.

(62) Hayes, G.; Biden, T. J.; Selbie, L. A.; Shine, J. Structural Subtypes of the Dopamine D2 Receptor Are Functionally Distinct: Expression of the Cloned D2A and D2B Subtypes in a Heterologous Cell Line. *Mol. Endocrinol.* **1992**, *6*, 920–926.

(63) Sokoloff, P.; Andrieux, M.; Besancon, R.; Pilon, C.; Martres, M. P.; Giros, B.; Schwartz, J. C. Pharmacology of Human Dopamine D3 Receptor Expressed in a Mammalian Cell Line: Comparison with D2 Receptor. *Eur. J. Pharmacol.* **1992**, *225*, 331–337.

(64) Asghari, V.; Sanyal, S.; Buchwaldt, S.; Paterson, A.; Jovanovic, V.; Van Tol, H. H. Modulation of Intracellular Cyclic AMP Levels by Different Human Dopamine D4 Receptor Variants. *J. Neurochem.* **1995**, *65*, 1157–1165.

(65) Hübner, H.; Haubmann, C.; Utz, W.; Gmeiner, P. Conjugated Enynes as Nonaromatic Catechol Bioisosteres: Synthesis, Binding Experiments, and Computational Studies of Novel Dopamine Receptor Agonists Recognizing Preferentially the D(3) Subtype. *J. Med. Chem.* **2000**, *43*, 756–762.

(66) Heindl, C.; Hübner, H.; Gmeiner, P. Ex-Chiral Pool Synthesis and Receptor Binding Studies of 4-Substituted Prolinol Derivatives. *Tetrahedron: Asymmetry* **2003**, *14*, 3141–3152.

(67) Lowry, O. H.; Rosebrough, N. J.; Farr, A. L.; Randall, R. J. Protein Measurement with the Folin Phenol Reagent. *J. Biol. Chem.* **1951**, *193*, 265–275.

(68) Cohen, F. R.; Lazareno, S.; Birdsall, N. J. The Effects of Saponin on the Binding and Functional Properties of the Human Adenosine A1 Receptor. *Br. J. Pharmacol.* **1996**, *117*, 1521–1529.

(69) Jiang, M.; Bajpayee, N. S. Molecular Mechanisms of Go Signaling. *Neurosignals* **2009**, *17*, 23–41.

(70) Hübner, H.; Kraxner, J.; Gmeiner, P. Cyanoindole Derivatives as Highly Selective Dopamine D_4 Receptor Partial Agonists: Solid-Phase Synthesis, Binding Assays, and Functional Experiments. *J. Med. Chem.* **2000**, *43*, 4563–4569.

(71) Bettinetti, L.; Schlotter, K.; Hübner, H.; Gmeiner, P. Interactive SAR Studies: Rational Discovery of Super-Potent and Highly Selective Dopamine D3 Receptor Antagonists and Partial Agonists. *J. Med. Chem.* **2002**, *45*, 4594–4597.

(72) Cheng, Y.; Prusoff, W. H. Relationship between the Inhibition Constant (K_i) and the Concentration of Inhibitor Which Causes 50% Inhibition (IC_{50}) of an Enzymatic Reaction. *Biochem. Pharmacol.* **1973**, *22*, 3099–3108.

(73) Kenakin, T.; Miller, L. J. Seven Transmembrane Receptors as Shapeshifting Proteins: The Impact of Allosteric Modulation and Functional Selectivity on New Drug Discovery. *Pharmacol. Rev.* **2010**, *62*, 265–304.

(74) Finn, A. K.; Whistler, J. L. Endocytosis of the mu Opioid Receptor Reduces Tolerance and a Cellular Hallmark of Opiate Withdrawal. *Neuron* **2001**, *32*, 829–839.

(75) Frisch, M. J.; Trucks, G. W.; Schlegel, H. B.; Scuseria, G. E.; Robb, M. A.; Cheeseman, J. R.; Zakrzewski, V. G.; Montgomery, J. A., Jr.; Stratmann, R. E.; Burant, J. C.; Dapprich, S.; Millam, J. M.; Daniels, A. D.; Kudin, K. N.; Strain, M. C.; Farkas, O.; Tomasi, J.; Barone, V.; Cossi, M.; Cammi, R.; Mennucci, B.; Pomelli, C.; Adamo, C.; Clifford, S.; Ochterski, J.; Petersson, G. A.; Ayala, P. Y.; Cui, Q.; Morokuma, K.; Malick, D. K.; Rabuck, A. D.; Raghavachari, K.; Foresman, J. B.; Cioslowski, J.; Ortiz, J. V.; Stefanov, B. B.; Liu, G.; Liashenko, A.; Piskorz, P.; Komaromi, I.; Gomperts, R.; Martin, R. L.; Fox, D. J.; Keith, T.; Al-Laham, M. A.; Peng, C. Y.; Nanayakkara, A.; Gonzalez, C.; Challacombe, M.; Gill, P. M. W.; Johnson, B.; Chen, W.; Wong, M. W.; Andres, J. L.; Head-Gordon, M.; Replogle, E. S.; Pople, J. A. *Gaussian 98*, revision A.7; Gaussian, Inc.: Pittsburgh, PA, 1998.

(76) Case, D. A.; Darden, T. A.; Cheatham; Simmerling, C. L.; Wang, J.; Duke, R. E.; Luo, R.; Crowley, M.; Walker, R. C.; Zhang, W.; Merz, K. M.; Wang, B.; Hayik, S.; Roitberg, A.; Seabra, G.; Kolossváry, I.; Wong, K. F.; Paesani, F.; Vanicek, J.; Wu, X.; Brozell, S. R.; Steinbrecher, T.; Gohlke, H.; Yang, L.; Tan, C.; Mongan, J.; Hornak, V.; Cui, G.; Mathews, D. H.; Seetin, M. G.; Sagui, C.; Babin, V.; Kollman, P. A. *AMBER 10*; University of California: San Francisco, CA, 2008.

(77) Hornak, V.; Abel, R.; Okur, A.; Strockbine, B.; Roitberg, A.; Simmerling, C. Comparison of Multiple Amber Force Fields and Development of Improved Protein Backbone Parameters. *Proteins* **2006**, *65*, 712–725.

(78) Bayly, C. I.; Cieplak, P.; Cornell, W.; Kollman, P. A. A Well-Behaved Electrostatic Potential Based Method Using Charge Restraints for Deriving Atomic Charges: The RESP Model. *J. Phys. Chem.* **1993**, *97*, 10269–10280.